DELFT UNIVERSITY OF TECHNOLOGY

DEPARTMENT OF AEROSPACE ENGINEERING

Memorandum M-274

The Calculation of RMS Values of Deviations of Aircraft Controlled to Fly Along a Desired Flight Path

by

J.C. van der Vaart

H.L. Jonkers

F.K. Kappetijn

Paper to be presented at the AGARD
Guidance and Control Panel Symposium
on Applications of Advances in Navigation
to Guidance and Control, 10-13 May 1977
Stuttgart, Germany

Delft - The Netherlands

April 1977

SUMMARY

This Paper gives a description of a method to calculate the covariance matrix, as a function of time, of a linear system perturbed by a number of random noise signals. Using basic principles of modern system theory it allows the computation of variances or r.m.s. values of aircraft variables in the case where system dynamics and statistical properties of the disturbing noise signals are a function of time.

Results are shown of a numerical example of the symmetric motions of a present day jet transport in a coupled approach followed by an automatic landing, the random disturbing signals being gaussian atmospheric turbulence and ILS electronic noise.

The problem of wind shear is briefly touched upon and an analytical approach to "worst case" wind time histories is presented.

TABLE OF CONTENTS

1. INTRODUCTION

One of the aims of the control of flight, be it manual or automatic, can be considered to be the reduction of the effects of external and internal disturbances acting on the controlled system i.e. the aeroplane.

These disturbances can be devided into two distinct categories, one being caused by malfunctions of any part of the controlled system, the other category being caused by signals of a random nature, resulting in errors relative to a desired state or trajectory while all parts of the system are functioning within specifications.

The first category of obvious malfunctions is left out of consideration here. The present Paper is only concerned with the class of random disturbances such as atmospheric turbulence, electronic and mechanical noise.

When designing or evaluating control systems it is important to be able to make estimates of the effects of these random signals on the performance of systems. Considering the disturbing signals as so called random processes and making a number of assumptions on these processes make them accessable to practical statistical calculations.

Assuming that the random processes under consideration are normal or gaussian and that the dynamic behaviour of the systems can be described by linear differential equations (system linearity) opens the road to a number of straightforward mathematical methods.

It should be mentioned that atmospheric turbulence, for example, can only approximately be described as a normal (gaussian) process. Attempts have been made by others to tackle the phenomenon of non-gaussian turbulence which is especially important in the field of flight simulation (Refs. 1 and 2).

When designing control systems for the purpose of reducing system sensitivity to disturbing signals it can often be assumed that noise processes are gaussian. The calculation method described in this Paper is based on such an assumption and on the one of system linearity. For the sake of completeness, it should be mentioned that it is, in principle, possible to treat non-linearities in a quasi-linear manner, see Ref. 3.

Statistical ensemble properties such as variances or r.m.s. levels of output signals of a system driven by a number of random noise signals can be devided in two classes. Steady state properties are namely clearly to be distinguished from transient properties. This is illustrated by Fig. 1 showing a system, initially at rest, perturbed by a random noise input signal from $t = 0$ onwards. The variance of the output signal, being zero at $t = 0$, grows through a transient response to its final or steady state if the system is stable.

Suppose for instance that one is interested to know r.m.s. levels or exceedance probabilities of normal accelerations, load factors, altitude or course deviations of an aircraft due to atmospheric turbulence in cruising flight. Here the statistical characteristics of turbulence as well as the dynamic properties of the aircraft can assumed to be constant and the r.m.s. levels and exceedance probabilities of interest can be considered as steady state properties. A number of well-established methods are available for such steady state problems (Refs. 4 and 5).

A quite different problem is best illustrated by the example of an aircraft in a coupled approach to land. Due to the decreasing altitude during the approach and the altitude dependent statistical properties of atmospheric turbulence, the aircraft experiences time-varying random turbulence. Moreover ILS glide path beam geometry may cause changes in effective gains of the glide slope coupler. Finally, if an automatic landing is carried out, the autopilot mode changes drastically while in this phase also the aerodynamic

characteristics change due to ground effects. Still one would like to calculate r.m.s. values of motion variables during the approach and landing, especially at certain instants in time such as at decision height and touch down.

Such a calculation could be carried out by a Monte Carlo simulation. Another method is the one using impulse responses in an analogue computation (Ref. 6). A much more accurate, straightforward and faster method using transient statistical properties is the one reviewed in the present Paper. Basicly it is an application of known elements of modern system theory and the concept as such can of course not be claimed to be entirely novel. A similar method, described in less detail, was apparently used in a plublication by Holley and Bryson (Ref. 7).

The purpose of this Paper is to give a practical example of some capabilities of modern system theory and it is to be hoped that it gives some guidance to control engineers faced with problems of a stochastic nature.

The main advantage of the method presented is perhaps that it permits statistical calculations on any linear system perturbed by gaussian random noise signals when either the statistical properties of the noise signals or the dynamics of the system, or both, are changing with time.

In the example mentioned earlier of an aircraft in the approach to land, the influence of altitude dependent properties of atmospheric turbulence can then be determined. Changes in electronic noise in the ILS signal during such an approach, gradual changes in autopilot gains and also the effect of a sudden decoupling of the autopilot are also easily studied in this way.

The present Paper gives an overview of the underlying theory and some results. A detailed description of the pertaining computer program is to be published shortly (Ref. 8). The second Chapter

illustrates, by some simple examples, the principle of using transient responses to obtain statistical properties of a time-varying system. Chapter 3 deals with the particular manner in which noise processes are to be modelled, followed by a survey in Chapter 4 of the numerical simulation of the aircraft, the autopilot, the atmospheric turbulence and the ILS noise process. Results of a number of calculations are given in Chapter 5.

Although the nature of the phenomenon usually denoted by the term "wind shear" is such that a statistical treatment appears hardly possible, this subject is briefly touched upon in Chapter 6. It is shown that deviations from a desired trajectory caused by certain, analytically derived, deterministic "worst case" wind time histories are proportional to statistical properties in a special case of stochastic wind signals. Some insight into the effects of worst case wind time histories (or windshears) might thus be gained using the calculation method that forms the main subject of this Paper.

2. THE TRANSIENT RESPONSE OF THE COVARIANCE MATRIX. SOME EXAMPLES.

This chapter gives a number of simple examples of the calculation of the transient response of statistical characteristics of output signals of a system driven by a white noise input signal. It will be shown how this calculation can be done in the case of time-varying properties of either the driving noise signal, the driven system itself or both. The Appendix contains a more detailed description.

Consider a dynamic system, initially at rest and driven by a random noise input signal $v(t)$ from $t = 0$ onwards, see Fig. 1. The variance σ_x^2 of the output signal x (or the r.m.s. value σ_x of x), being zero at $t = 0$, will reach a steady state level in a finite time if the system is stable, Fig. 1a. The steady state value can be calculated by a number of methods, for instance by a frequency domain technique. The transient response can only be calculated by time domain techniques such as the one described in this Paper or by a time consuming Monte Carlo simulation in which a large number of replications is taken, the system being at rest initially for each replication.

If the random input signal is switched off after the steady state has been reached, the variance of x returns to zero after another transient, Fig. 1b. This transient is identical with the one that would be obtained if $v(t)$ were zero for all t, the initial condition being equal to the steady state value of σ_x^2.

In modern system theory the more important statistical quantities are expressed by the covariance matrix $C_{xx}(t)$ of the state vector $\underline{x}(t)$ of the system under consideration. In the case of an aircraft the state vector $\underline{x}(t)$ is the vector of the motion variables, and the covariance matrix then contains the variances of the motion variables as the diagonal elements and the covariances as the off-diagonal elements.

Next, by way of example, a simple second order system such as the mass-spring-dashpot combination of Fig. 2 is considered. The state

vector $\underline{x}(t)$ is

$$\underline{x}(t) = \begin{bmatrix} x_1(t) \\ x_2(t) \end{bmatrix}$$

where $x_1(t) = d(t)$ and $x_2(t) = \dot{d}(t)$.

The covariance matrix of the state vector $\underline{x}(t)$ is then:

$$C_{xx}(t) = \begin{bmatrix} c_{11}(t) & c_{12}(t) \\ c_{21}(t) & c_{22}(t) \end{bmatrix} = \begin{bmatrix} \sigma_{x_1}^2(t) & \sigma_{x_1x_2}(t) \\ \sigma_{x_2x_1}(t) & \sigma_{x_2}^2(t) \end{bmatrix} \quad (1)$$

Now according to the Appendix $C_{xx}(t)$ consists of two terms:

$$C_{xx}(t) = D_{xx}\{C_{xx}(0),t\} + E_{xx}\{w(t),t\} \quad (2)$$

The two terms in eq. (2) represent the two different responses just mentioned. The first term D_{xx} gives the response to the initial conditions $C_{xx}(0)$, the second term E_{xx} is an expression for the response to a white noise input signal $w(t)$ acting on the system.

Fig. 3 shows the response of each element of $C_{xx}(t)$ caused by a white noise signal acting on the second order system of Fig. 2 from $t = 0$ onwards, initial conditions $C_{xx}(0)$ being zero. The responses are shown for different values of the damping ratio ζ. It can be seen that the covariances of x_1 and x_2 become zero in the steady state, a peculiarity of this example, where x_2 is the time-derivative of x_1.

In Fig. 4 the response to unit initial conditions is given (first right hand term of eq. (2)). Fig. 5 shows the response caused by a white noise signal of limited duration (5 secs). The responses from $t = 5$ onwards are given by the term D in eq. (2) by setting the initial conditions of C_{xx} at the values at $t = 5$.

Calculating the transient response to a noise signal of limited duration opens the possibility of determining the response to an input noise signal with time-varying statistical properties. If it is known how these properties are changing with time, the response can be determined as illustrated in Fig. 6, where the intensity of the input signal is increased at t = 5.

Fig. 7 shows an example where one of the systems' characteristics, the damping ratio ζ, changes from 0.7 to 0.2 at t = 8 sec. As in Fig. 6, the total response after the change is obtained as the sum of the terms D and E of eq. (2), the initial conditions in D being set at the values of the elements of $C_{xx}(t)$ reached up to that moment.

In the examples of Figs. 5, 6 and 7 the instants in time at which the changes in input signal and damping ratio occur were, for the benefit of simplifying the figures chosen such that steady states had been reached. This is of course not necessary.

From the examples of this Chapter it will be evident that the covariance matrix, as a function of time in the case of gradually changing system or input characteristics, can be calculated by approximating these changes by small, stepwise variations. Details of the modelling and the calculation of responses to coloured noise signals will be dealt with in the next Chapters.

3. MODELLING THE AIRCRAFT AND THE NOISE PROCESSES

The examples in the foregoing Chapter were of systems perturbed by white noise processes. The theory on which the calculation of the covariance matrix is based indeed assumes a system driven by one or more white noise signals. These idealized processes do not occur in reality. The coloured noise processes such as atmospheric turbulence and electronic noise are therefor usually modelled such that they can be thought to be obtained by the filtering of white noise. The technique to mathematically derive the differential equations and the transfer functions of these shaping filters is well established. Details can be found in Ref. 5.

The numerical example, of which details will be given in the next Chapter, is of the symmetric motions of an aircraft in a coupled approach, followed by an automatic landing manoeuvre. The noise processes considered are horizontal and vertical turbulence and ILS glide slope electronic noise. The block diagram of Fig. 8a gives the arrangement of the shaping filters and the aircraft plus autopilot.

The box in Fig. 8a denoted by "observation process" would represent a pure summation in classic control theory if there is no observation noise. Apart from ILS noise, no observation noise was assumed to be present in the example of this Paper.

If the shaping filters are next joined to the aircraft, as visualized in Fig. 8b, one system perturbed by a number of white noise signals is obtained, see Fig. 8c. Mathematically this operation is achieved by combining the differential equations of the shaping filters with the aircraft's state equations to obtain the augmented state equations, see the Appendix.

One remark should be made on the modelling of the atmospheric turbulence. Generating the coloured noise representing atmospheric turbulence velocities by filtering white noise is only possible if the power spectral densities have a rotional form. The well known Dryden spectra used

in the example, indeed fulfill this condition.

The Von Karman spectra in contrast, have no rational form and can only be approximated by linear filters. An alternative, exact method to calculate the covariance matrix for a given correlation function of a coloured noise input signal is briefly treated in the Appendix. This enables carrying out calculations as the ones described in this Paper, using atmospheric turbulence as characterized by the Von Karman correlation functions or power spectra.

Now that in the second Chapter the principle of statistical calculations for a time-varying system have been dealt with and the equations have been arranged in the proper form it seems worthwhile to summarize the changes in statistical properties of input signals and changes in the dynamics of the system itself that can now be studied.

First the level of atmospheric turbulence or the ILS noise can be altered either by changing the intensity of the white noise input signals or by changing the gain in the filter transfer functions.

Further the shape of the power spectrum of the atmospheric turbulence may be altered by changing the appropriate parameters (integral scale lengths).

Next changes in the autopilot can be modelled, such as the gradually changing gain due to glide path beam geometry. When performing an automatic landing, the effect of the changing operating mode of the autopilot on the statistics of deviations from an ideal trajectory can be evaluated. Also in the landing phase changes in aerodynamic properties due to ground effects can be modelled by changing the appropriate aerodynamic coefficients.

Another possibility is to study the effect of a sudden decoupling of autopilot or autothrottle. Finally it will, in principle be possible to evaluate programmed changes in aircraft configuration for instance flap settings or power settings as required for decelerated or two-segment approaches.

4. DETAILS OF THE NUMERICAL EXAMPLE

To illustrate the capabilities of the calculation method it has been applied to a numerical example of a present day, four engined, subsonic jet transport in a coupled approach followed by an automatic landing. Details of the aircraft, the autopilot and autothrottle gain settings for the coupled approach and for the automatic landing can be found in Refs. 5 and 9. No efforts have been made to optimize the autopilot according to some criterion. Although the layout and the gain settings of the autopilot do not represent any existing installation, they can be considered to represent the present state of the art.
In order to calculate, in the landing phase, the variances and covariances of deviations relative to an average landing flare, small perturbation equations of motions relative to an ideal, unperturbed automatic landing flare have been used. The ground effect during the flare was also modelled as a small perturbation effect due to deviations from the (known) ideal landing flare.

The atmospheric turbulence, acting during the approach down to flare initiation, was characterized by the Dryden spectra (Ref. 10). The integral scale lengths and turbulence intensity were chosen according to the model of Pritchard (See Ref. 10) for a neutral atmosphere, see Fig. 9. The wind speed at reference height (9.15 m) was chosen at 1 m/sec (approx. 2 knots) in most of the examples.

The terrain factor R_T was chosen at 1,1 (flat agricultural land) resulting in turbulence that could be considered "light" (standard deviation 0,5 m/sec approx. at 200 m altitude). Under the assumption of system linearity, the results computed can be readily extrapolated for more severe turbulence intensities.

The ILS noise intensity, see Fig. 10, and scale length were those specified for CAT I (Ref. 10).

Two cases of changes in gain due to glide slope beam geometry were

considered. In one case the gain, expressed by elevator angle per degree angular deviation from the glide path, was taken to decrease exponentially in two distinct phases as shown in Fig. 11, representing a realistic example of a practically implemented compensation. The result is a nearly constant effective gain (elevator angle per foot deviation from the glide path), see Fig. 11.

In another case, no compensation was assumed, resulting in an increasing effective gain as the aircraft approaches the threshold.

All these gradually changing gains, coefficients, intensities etc. were approximated by stepwise variations in time, the entire white noise driven system remaining constant during relatively short time intervals.

5. SOME RESULTS

In Figs. 13, 14 and 15 some results are given of the calculation of variances, due to atmospheric turbulence only, of deviations from the glide path and from an ideal flare, see Fig. 12.
Variances of flight speed, altitude deviations and sink rate can be seen to decrease due to the decreasing intensity of the turbulence and the decreasing integral scale length.

A decreasing scale length is to be seen as a shift in the maximum level of the power spectrum to higher frequencies.
If the aircraft is considered as a low pass filter, a decreasing scale length has a tendency to decrease the variance of aircraft output signals.

Also shown in Figs. 13, 14 and 15 is the effect of a sudden decoupling of the autopilot at 40 seconds to touchdown.
The subsequent growth in variances shown supposes no corrective action by a pilot. The periodic nature of the responses of the variances of flight speed and sink rate is due to the fact that the natural motions of the unstabilized aircraft are of course much more lightly damped than those of the tightly controlled aircraft in the coupled approach. Still the variance of the flight speed and sink rate can be seen to decrease in the long run as the unstabilized, free aircraft is stable with respect to flight speed and sink rate, which is not the case with respect to altitude.
It can be seen from Fig. 14 that the variance of altitude is increasing after decoupling due to the indifferent or neutral stability of the free aircraft with respect to altitude.

An interesting result can be observed if atmospheric turbulence is made to occur during the last 30 secs. only, see Figs. 13, 14 and 15.
It can be concluded that deviations at a certain instant in time (say at decision height, flare height or touchdown) can, for a well damped aircraft, be considered to be mainly caused by the turbulence during the preceding 20 to 30 seconds.

In Fig. 16 the variance of the altitude deviations caused by ILS noise only is given. The effect of this at decision height or touchdown can be seen to be roughly equal to the effect of moderate turbulence. It will be evident that the variance of altitude deviations caused by ILS noise will never be less than the variance of the noise of the ILS reference signal itself if expressed in altitude deviations, (see also Fig. 10), as no prefiltering of the ILS signal was presumed.

The effect of the (non-ideal) compensation of Fig. 11 turned out to be small. To more dramatically illustrate the ability of the computation method to cope with the effect of changing gains, or more generally with changing dynamic system properties, another example is given in Fig. 17.

A change in effective gain, if not compensated at all, is shown in the top figure of Fig. 17. For a modern transport aircraft this change is perhaps less realistic but it can be considered to be representative of general aviation autopilots where the gain with respect to angular deviation from the glide path, is constant. Obviously the aircraft is becoming less stable from approximately 20 seconds to touchdown onwards.

Apart from deviations in flight speed, altitude and sink rate, another important parameter is of course the deviation Δx in distance along the runway, at a certain fixed altitude, relative to an ideal, undisturbed approach path and flare trajectory. The along the runway deviations are related to the deviation relative to the glide path by the simple relation depicted in Fig. 12. For along the runway scatter of touchdown point the influence of the changing value of the flight path angle γ should be taken into account.

Finally it will be evident that the present method has possible applications in the field of 4-D navigation. The variance of the deviation along the flight path can be computed by including this deviation as an element in the aircraft's state vector. In this way the variance of the time of arrival at a certain point in space is easily established.

6. WORST CASE WINDSHEARS

Statistical calculations of aircraft motions in moving air are based on the usual mathematical models of atmospheric turbulence such as the Von Karman or Dryden power spectra mentioned before.

There are a number of atmospheric phenomena that are not, or not properly accounted for in these statistical models. For example more or less stationary mean wind gradients or shears may occur, causing a descending or climbing aeroplane to experience relatively slowly changing wind speeds and directions. Deterministic models of mean wind speed as a function of altitude under certain meteorological conditions are available (Ref. 10), but there are still more atmospheric phenomena that are not properly represented in the statistical models.

It is well known, especially at low altitudes, where the intensity of random atmospheric turbulence according to the usual models should be low, strongly changing winds due to special terrain features or buildings may be met with. Thermals in, apart from that, quiet conditions or more obviously downdraughts in thunderstorms may induce hard landings or even worse. Some or all of these low frequency turbulence phenomena at low altitudes are also sometimes less correctly referred to as "wind shears".

Apart from the deterministic mean wind gradients mentioned above, there is as yet no means of realistically modelling the statistical characteristics of the entire class of low altitude, low frequency turbulence.

One way to gather some understanding of aircraft motions due to low frequency turbulence is to theoretically study aircraft motions caused by actually recorded wind time-histories of a notoriously unfavourable character. Another way is trying to find, according to some criterion, the particular deterministic wind (or turbulence) time-history that causes the greatest deviation of one of the motion

variables relative to an ideal course.

Corbin (Ref. 11) derived such worst case turbulence time histories by a search procedure yielding "worst" combinations of a number of sines and cosines.

It appears, however, that worst case time histories can also be found by a more analytical approach. The following is a brief description of attemps made by the authors of this Paper to describe the worst cases in terms of linear system theory.

This concept, of which a more formal derivation is to be given in Ref. 12, can be illustrated by a simple example.

The response of one particular state or motion variable x_i of the state $\underline{x}(t)$ of a constant linear system on one single input signal $v(t)$ if the system is at rest initially can be written as (See Ref. 13):

$$x_i(t) = \int_0^t h_i(t - \tau) \cdot v(\tau) \cdot d\tau \qquad (3)$$

where $h_i(t)$ is the response of x_i to a unit impulse $\delta(o)$ at $t = 0$.

The integral according to eq. (3) has been visualized in Fig. 18. The function $h_i(t - \tau)$, being the time reversed impulse response of x_i from t to τ, can be considered as a measure of the contribution of v at instant τ, to the value of x_i at t.

Without a formal derivation it can easily be seen from eq. (1) and from Fig. 18 that it is plausible that, for a given fixed value of t, the absolute value of $x_i(t)$ will be maximal if $v(\tau)$ is exactly proportional to $h_i(t - \tau)$ for all τ. In other words the worst case time-history of $v(t)$, to obtain a maximum deviation of $x_i(t)$ is proportional to the time reversed impulse response of x_i:

$$v(\tau) = C \cdot h_i(t - \tau) \tag{4}$$

where C is a constant.

Now consider a system with a number of output signals such as an aircraft, then all output signals (or motion variables) have different impulse responses. As a consequence there will be one particular worst case input signal for each of the output variables.

Fig. 19 gives two such worst case time histories of the horizontal wind velocity and the resulting largest deviations of altitude and sink rate. The deviations were calculated by generating the response of the (unstabilized) example aircraft by solving the governing differential equations for the given input time histories.

It can be seen that maximum wind excursions of only 1 m/sec (2 knots approximately) in both cases, induced an altitude loss of 25 m (80 ft) in one case and an excess sink rate of 2.3 m/sec (450 ft/min) in the other. As already mentioned the aircraft was not stabilized in this case and no pilot action was supposed to be involved. As a vigilant pilot would of course take immediate corrective action, the example represents a worst case in more than one sense.

Apart from solving the governing differential equations for the given worst input time histories there is still another way to obtain the values of the maximum deviations, which can be shown as follows. Substituting eq. (4) into eq. (3) yields:

$$x_i(t) = C \int_o^t h_i^2(t - \tau)\, d\tau \tag{5}$$

By considering Fig. 18 it is easily seen that this is equal to:

$$x_i(t) = C \int_o^t h_i^2(t) \cdot dt \tag{6}$$

Now it has been shown elsewhere, see Ref. 5, that the integral in eq. (6) is equal to the variance at t of the output signal $x_i(t)$ if

the system under consideration is perturbed by a white noise random input signal w(t), with intensity equal to C, from t = 0 onwards:

$$\sigma_{x_i}^2 = C \int_0^t h_i^2(t)\, dt$$

Thus the maximum deviation of x_i at time t, caused by its particular deterministic, worst case input signal is seen to be equal to the variance $\sigma_{x_i}^2(t)$ in the stochastic case where the system is perturbed by a white noise signal with intensity C:

$$x_i(t) = \sigma_{x_i}^2(t)$$

This result has been visualized in the diagram of Fig. 20.

As regards the non-maximum deviation of some other motion variable for instance $x_j(t)$, due to the particular deterministic input signal causing the largest deviation of x_i at t, it can be shown that $x_j(t)$ is equal to the covariance $\sigma_{x_i x_j}(t)$ of $x_i(t)$ and $x_j(t)$ in the stochastic case just mentioned. The problem of finding all deviations caused by any particular worst case time history is thus reduced to calculating the covariance matrix of the state vector of a linear system perturbed by one white noise input signal.

The tentative concept of worst case wind time histories as briefly summarized above, could be used as a tool to evaluate the sensitivity of given aircraft control systems to the class of low frequency atmospheric turbulence broadly described as wind shears.

In the case of an automatic landing, the analytic concept of worst case wind time histories should be extended to account for changing system characteristics. It appears that this could be achieved by defining worst case initial conditions for the deterministic case and establishing a relation with the response to initial conditions of the covariance matrix in the stochastic case.

7. CONCLUDING REMARKS

For the calculation of variances or r.m.s. levels of output variables of a time-varying noise driven system advantage can be taken of concepts of modern system theory. Using a computation method as described in this Paper it is possible to avoid relatively inaccurate and time comsuming Monte Carlo simulations.

The method described can also be adapted such that input signals, characterized by given correlation functions, can be used. This enables an exact representation of the Von Karman turbulence spectra. Approximating these spectra by linear filtering can thus be avoided.

Finally it may be obvious that the formulation in terms of system theory concepts is such that it opens possibilities for the design of control systems by optimization techniques.

As to the worst case windshears discussed in Chapter 5 only some tentative conclusions appear to be appropriate at the present moment. Of course any so called "worst case" wind time history is only worst according to the criterion chosen. The concept of interpreting the time-reversed impulse response as a measure for the contribution at a certain altitude to deviations at decision height or touchdown seems an attractive one and moreover, the computation of maximum deviations obtained is straightforward. For automatic approaches, followed by an automatic landing, in which case the system's dynamic properties change with time, the method should be extended in the way of defining "worst case" initial conditions.

8. REFERENCES

1. G.A.J. van de Moesdijk — Simulation of patchy atmospheric turbulence, based on measurements of actual turbulence. AGARD-CP-198 on Flight simulation/Guidance systems simulation, 1975.

2. B.N. Tomlinson — Developments in the simulation of atmospheric turbulence.AGARD-CP-198 on Flight simulation/Guidance systems simulation, 1975.

3. K. Sidwell — A method for the analysis of non-linearities in aircraft dynamic response to atmospheric turbulence, NASA TN D-8265 (1976).

4. O.H. Gerlach — Calculation of the response of an aircraft to random atmospheric turbulence. Part I - Symmetric motions. Report VTH-138. Technological University Delft, Department of Aeronautical Engineering, 1966.

5. J.C. van der Vaart — The impulse response method for the calculation of statistical properties of aircraft flying in random atmospheric turbulence. Report VTH-197. Delft University of Technology, Department of Aerospace Engineering, 1975.

6. O.H. Gerlach, G.A.J. van de Moesdijk, J.C. van der Vaart — Progress in the mathematical modelling of flight in turbulence. AGARD-CP-140 on Flight in Turbulence, 1973.

7. W.E. Holley, A.E. Bryson — Wind modeling and lateral control for automatic landing. Journal of Spacecraft and Rockets, Vol. 14, no. 2, Febr. 1977.

REFERENCES (continued)

8. H.L. Jonkers, F.K. Kappetijn, J.C. van der Vaart — Digital calculation of the propagation in time of the aircraft gust response covariance matrix. Report LR. Delft University of Technology, Department of Aerospace Engineering (to be published).

9. J.C. van der Vaart — De automatische afvangmanoeuvre van een verkeersvliegtuig (the automatic landing flare of a transport aircraft, in Dutch). Report VTH-182, Delft University of Technology, Department of Aeronautical Engineering, 1974.

10. — AGARD Report no. 632 on Approach and Landing Simulation, 1975.

11. M.J. Corbin — Turbulence time-histories causing greatest touchdown errors following an automatic flare. Tech. Memo Avionics 152, Royal Aircraft Establishment, 1973.

12. J.C. van der Vaart — Worst case wind time-histories causing largest deviations from a desired flight path. An analytical approach. Report LR. Delft University of Technology, Department of Aerospace Engineering (to be published).

13. H. Kwakernaak, R. Sivan — Linear optimal control systems. Wiley-Interscience, Inc. New York, London, Sydney, Toronto, 1972.

14. H.L. Dryden, S.K. Friendlander, L. Topper — Review of the statistical theory of turbulence.In: Classic papers on statistical theory, Interscience Publ. Inc., New York, 1961.

REFERENCES (continued)

15. A.P. Sage
J.L. Melsa
Estimation theory with applications to communications and control, McGraw-Hill, New York, 1971.

APPENDIX

THE COMPUTATION OF THE COVARIANCE MATRIX AS A FUNCTION OF TIME

The problem of computing variances and covariances of aircraft response to atmospheric turbulence can be reduced to computation of the corresponding response statistics of a linear system driven by zero mean, gaussian, white noise, if:

1. the atmospheric perturbations are assumed zero mean and normally distributed,
2. the atmospheric perturbations are assumed small enough to justify linearization of the aircraft's aerodynamics and the aircraft's equations of motion,
3. Taylor's frozen field hypothesis is assumed valid, i.e. if the aircraft's mean airspeed is assumed large as compared to the rate of changes in atmospheric motions.

Prior to embarking on the explanation of the solution of this problem, it should be remarked that the method applied includes utilization of the atmospheric turbulence autocovariance functions published by H.L. Dryden, see Friedlander and Topper (Ref. 14). An alternative and more general method not depending on the Dryden autocovariance functions is also presented.

The state equation

Considering the aircraft's symmetric motions and using:

1. the state variables:

$$\hat{u}(t),\ \alpha(t),\ \theta(t),\ \frac{q(t)\ \bar{c}}{V_o},\ h(t),\ H(t),\ T_c(t) \text{ and } \Delta x(t),$$

2. the control variables:

$$\delta_e(t) \text{ and } T_{c_i}(t),$$

3. the gust velocity components and their time derivatives:

$\hat{u}_g(t)$, $\alpha_g(t)$, $\dot{\hat{u}}_g(t)$ and $\dot{\alpha}_g(t)$,

the following set of linearized equations of motion can be formulated to describe the dynamics of an aircraft in atmospheric turbulence.

$$2\mu_c D_c \hat{u}(t) = C_{X_u}\hat{u}(t) + C_{X_\alpha}\alpha(t) + C_{Z_o}\theta(t) + \Delta C_{X_h}(t)h(t) \tag{A.1}$$

$$2\mu_c D_c \alpha(t) = C_{Z_u}\hat{u}(t) + C_{Z_\alpha}\alpha(t) - C_{X_o}\theta(t) + (C_{Z_q} + 2\mu_c)\frac{q(t)\,\bar{c}}{V_o} +$$

$$+ \Delta C_{Z_h}(t)h(t) + C_{Z_\delta}\delta_e(t) + C_{Z_{u_g}}\hat{u}_g(t) +$$

$$+ C_{Z_{\alpha_g}}\alpha_g(t) + C_{Z_{\dot{u}_g}} D_c\hat{u}_g(t) + C_{Z_{\dot{\alpha}_g}} D_c\alpha_g(t) \tag{A.2}$$

$$D_c\theta(t) = \frac{q(t)\,\bar{c}}{V_o} \tag{A.3}$$

$$2\mu_c K_Y^2 D_c \frac{q(t)\,\bar{c}}{V_o} = C_{m_u}\hat{u}(t) + C_{m_\alpha}\alpha(t) + C_{m_{\dot{\alpha}}} D_c\alpha(t) +$$

$$+ C_{m_q}\frac{q(t)\,\bar{c}}{V_o} + \Delta C_{m_h}(t)h(t) + C_{m_\delta}\delta_e(t) +$$

$$+ C_{m_{u_g}}\hat{u}_g(t) + C_{m_{\alpha_g}}\alpha_g(t) + C_{m_{\dot{u}_g}} D_c\hat{u}_g(t) +$$

$$+ C_{m_{\dot{\alpha}_g}} D_c\alpha_g(t) \tag{A.4}$$

$$D_c\frac{h(t)}{\bar{c}} = -\alpha(t) + \theta(t) \tag{A.5}$$

$$D_c\frac{V_o}{\bar{c}^2}H(t) = \frac{1}{\bar{c}}h(t) \tag{A.6}$$

$$D_c T_c(t) = -\frac{\bar{c}}{V_o\,\tau_{eng}}T_c(t) + \frac{\bar{c}}{V_o\,\tau_{eng}}T_{c_i}(t) \tag{A.7}$$

$$D_c\frac{\Delta x(t)}{\bar{c}} = \hat{u}(t) \tag{A.8}$$

Introducing:

1. the state vector:

$$\underline{x} \triangleq \text{col}\left(\hat{u},\ \alpha,\ \theta,\ \frac{q\bar{c}}{V_o},\ h,\ H,\ T_c,\ \Delta x\right), \tag{A.9}$$

2. the control vector:

$$\underline{u} \triangleq \text{col } (\delta_e, T_{c_i}), \tag{A.10}$$

3. the perturbation vector:

$$\underline{V}_g \triangleq \text{col } (\hat{u}_g, \alpha_g), \tag{A.11}$$

the equations of motion can be combined to formulate a first order linear vector matrix differential equation:

$$M_o D_c \underline{x}(t) = M_1 D_c \underline{x}(t) + M_2(t)\underline{x}(t) + M_3 \underline{u}(t) + M_4 \underline{V}_g(t) + M_5 D_c \underline{V}_g(t) \tag{A.12}$$

or:

$$\dot{\underline{x}}(t) = A(t)\underline{x}(t) + B\underline{u}(t) + C\underline{V}_g(t) + D\dot{\underline{V}}_g(t) \tag{A.13}$$

The matrices M_o, M_1, ..., M_5 can be specified by comparison of eqs. A.1 through A.11 with eq. A.12.

The observation equation

The quantities $\hat{u}_{a_m}^{*}(t)$, $\alpha_{a_m}(t)$, $\theta_m(t)$, $\frac{q_m(t)\,\bar{c}}{V_o}$, $h_m(t)$ and $H_m(t)$ can be considered as system output signal perturbations. Taking account of noisy ILS observations, these quantities are related to the state vector $\underline{x}(t)$, the atmospheric perturbation vector $\underline{V}_g(t)$ and ILS observation noise, writing:

$$\hat{u}_{a_m}(t) = \hat{u}(t) + \hat{u}_g(t) \tag{A.14}$$

---

* the suffix "a" is used to denote quantities, defined relative to the surrounding air-mass.
the suffix "m" is used to indicate measured magnitudes of the corresponding variables.

$$\alpha_{a_m}(t) = \alpha(t) + \alpha_g(t) \tag{A.15}$$

$$\theta_m(t) = \theta(t) \tag{A.16}$$

$$\frac{q_m(t)\,\bar{c}}{V_o} = \frac{q(t)\,\bar{c}}{V_o} \tag{A.17}$$

$$h_m(t) = h(t) + h_{gp}(t) \tag{A.18}$$

$$H_m(t) = H(t) + H_{gp}(t) \tag{A.19}$$

Introducing the output signal perturbation vector:

$$\underline{y} \triangleq \text{col}\ (\hat{u}_{a_m},\ \alpha_{a_m},\ \theta_m,\ \frac{q_m\,\bar{c}}{V_o},\ h_m,\ H_m) \tag{A.20}$$

and the ILS noise vector:

$$\underline{v} \triangleq \text{col}\ (h_{gp},\ H_{gp}) \tag{A.21}$$

the observation equations A.14 through A.19 can be combined to yield the vector matrix observation equation:

$$\underline{y}(t) = E\underline{x}(t) + F\underline{V}_g(t) + G\underline{v}(t) \tag{A.22}$$

The output equation

The variables of interest when analyzing the effects of atmospheric turbulence and ILS noise on an aircraft following the ILS glide slope are $\hat{u}(t)$, $\hat{u}_a(t)$, $h(t)$, $\Delta x(t)$ and $\Delta\dot{h}(t)$, where

$$\Delta\dot{h}(t) = V_o \sin\gamma(t)$$

$$\approx V_o(\theta(t) - \alpha(t)) \tag{A.23}$$

Defining:

$$\underline{z} \triangleq \text{col}\ (\hat{u},\ \hat{u}_a,\ h,\ \Delta x,\ \Delta\dot{h}) \tag{A.24}$$

the following vector matrix equation can be formulated:

$$\underline{z}(t) = R\underline{x}(t) + S\underline{V}_g(t) \tag{A.25}$$

The atmospheric turbulence

The random atmospheric perturbations acting upon the aircraft during flight in turbulence are often considered normally distributed, zero mean, and sequantially correlated with autocovariance functions:

$$C_{\hat{u}_g\hat{u}_g}(\tau) = \sigma_{\hat{u}_g}^2 \, e^{-\frac{V_o}{L_{u_g}}|\tau|} \tag{A.26}$$

$$C_{\alpha_g\alpha_g}(\tau) = \sigma_{\alpha_g}^2 \, e^{-\frac{V_o}{L_{w_g}}|\tau|} \left(1 - 2\frac{V_o}{L_{w_g}}|\tau|\right) \tag{A.27}$$

see Ref. 14.

Under these assumptions the atmospheric turbulence velocity components may be modelled as stochastic outputs of linear, low pass filters driven by gaussian, zero mean, white noise. Mathematical expressions for these filters can be derived using conventional Fourier transform techniques.

Specifying two white noise input processes $w_{11}(t)$ and $w_{12}(t)$ with unit intensity, the following mathematical expressions are obtained for the filters required:

$$\dot{\hat{u}}_g(t) = -\frac{V_o}{L_{u_g}(t)}\hat{u}_g(t) + \sigma_{\hat{u}_g}(t)\sqrt{\frac{2}{V_o L_{u_g}(t)}}\, w_{11}(t) \tag{A.28}$$

$$\dot{\alpha}_g(t) = \alpha_g^*(t) + \sigma_{\alpha_g}(t)\sqrt{\frac{3}{V_o L_{w_g}(t)}}\, w_{12}(t) \tag{A.29}$$

$$\dot{\alpha}_g^*(t) = -\frac{2V_o}{L_{w_g}(t)}\alpha_g^*(t) - \frac{V_o^2}{L_{w_g}^2(t)}\alpha_g(t) + \sigma_{\alpha_g}(t)\frac{1}{L_{w_g}(t)}\sqrt{\frac{V_o}{L_{w_g}(t)}}\,(1 - 2\sqrt{3})\, w_{12}(t) \tag{A.30}$$

or:

$$\dot{\underline{V}}_g^*(t) = P(t)\,\underline{V}_g^*(t) + Q(t)\,\underline{w}_1(t) \tag{A.31}$$

where

$$\underline{V}_g^* \triangleq \text{col}\ (\tilde{u}_g,\ \alpha_g,\ \alpha_g^*) \tag{A.32}$$

and:

$$\underline{w}_1 \triangleq \text{col}\ (w_{11},\ w_{12}) \tag{A.33}$$

The vector-valued quantity $\underline{V}_g(t)$ occurring in eqs. A.13 and A.22 can be related to the quantity $\underline{V}_g^*(t)$, see eq. A.31 writing:

$$\underline{V}_g(t) = T\,\underline{V}_g^*(t) \tag{A.34}$$

Glide path observation noise

Glide path observation errors may be described in terms of a normally distributed, zero mean, sequentially correlated random process with given autocovariance function:

$$Ch_{gp}h_{gp}(\tau) = \sigma_{gp}^2\, e^{-\frac{V_o}{L_{gp}}|\tau|} \tag{A.35}$$

see Ref. 10.

In a similar manner as shown for the atmospheric turbulence glide path observation noise can be considered as a outputsignal of a low pass filter, driven by gaussian, zero mean, white noise with unit intensity

$$\dot{h}_{gp}(t) = -\frac{V_o}{L_{gp}}\,h_{gp}(t) + \sigma_{h_{gp}}(t)\sqrt{\frac{2V_o}{L_{gp}}}\,w_2(t) \tag{A.36}$$

$$\dot{H}_{gp}(t) = h_{gp}(t) \tag{A.37}$$

where $H_{gp}(t)$ is the integrated glide path observation noise, specified in eq. A.36 and A.37.

Using the vector-valued quantity $\underline{v}(t)$, defined by eq. A.21 this filter expression can be written:

$$\dot{\underline{v}}(t) = M\underline{v}(t) + N(t)\, w_2(t) \tag{A.38}$$

The augmented state equation

Relating the control signal $\underline{u}(t)$ to the system output signal $\underline{y}(t)$, according to the control law

$$\underline{u}(t) = -K(t)\, \underline{y}(t) \tag{A.39}$$

where the gain $K(t)$ is prespecified and combining the eqs. A.13, A.22 and A.34 the following system state equation can be obtained:

$$\dot{\underline{x}}(t) = \left[A - BK(t)E\right] \underline{x}(t) + \left[CT + DTP(t) - BK(t)F\right] \underline{v}_g^*(t) - BK(t)G\underline{v}(t) + DTQ(t)\, \underline{w}(t) \tag{A.40}$$

Substitution of eq. A.34, in eq. A.25 yields the following result:

$$\underline{z}(t) = R\underline{x}(t) + ST\underline{V}_g^*(t) \tag{A.41}$$

Defining the augmented system state:

$$\underline{x}^* \triangleq \text{col}\ (\underline{x}, \underline{V}_g^*, \underline{v}) \tag{A.42}$$

and the white noise system input:

$$\underline{w} \triangleq \text{col}\ (\underline{w}_1, w_2) \tag{A.43}$$

with unit intensity, the eqs. A.31, A.38, A.40 and A.41 can be rearranged to yield:

$$\dot{\underline{x}}^{*}(t) = A^{*}(t)\ \underline{x}^{*}(t) + B^{*}(t)\ \underline{w}(t) \tag{A.44}$$

$$\underline{z}(t) = D^{*}\underline{x}^{*}(t) \tag{A.45}$$

Computation of the covariance matrix

The system state covariance matrix $C_{xx}(t)$ can be found solving the following equation:

$$\dot{C}_{xx}(t) = A^{*}(t)C_{xx}(t) + C_{xx}(t)A^{*}(t)^{T} + B^{*}(t)VB^{*}(t)^{T} \tag{A.46}$$

with the initial condition $C_{xx}(t_o)$ and where V is the unit matrix. Solving eq. A.49 yields:

$$C_{xx}(t) = \Phi(t,t_o)C_{xx}(t_o)\Phi(t,t_o)^{T} + \int_{t_o}^{t} \Phi(t,\tau)B^{*}(\tau)VB^{*}(\tau)^{T}\Phi(t,\tau)^{T}d\tau \tag{A.47}$$

$$= D_{xx}\{C_{xx}(t_o),t\} + E_{xx}\{w(t),t)\} \tag{A.48}$$

where $D_{xx}(t)$ is the covariance matrix of the system response at time t on the initial condition $C_{xx}(t_o)$ and $E_{xx}(t)$ denotes the covariance of the systemresponse on the white noise input $w(\tau)$ for $t_o \leq \tau \leq t$. For computation of the solution of this equation the problem is discretized in time. This implies that the systemmatrices $A^{*}(t)$ and $B^{*}(t)$ are assumed piecewise constant for $t_{k-1} \leq t < t_k$, for k = 1, 2, ... The solution obtained can then be formulated as:

$$C_{xx}(t_k) = \Phi(t_k,t_{k-1})\ C_{xx}(t_{k-1})\ \Phi(t_k,\ t_{k-1})^{T} +$$

$$+ \Gamma(t_k,\ t_{k-1})\ V_k\ \Gamma\ (t_k,\ t_{k-1})^{T} \tag{A.49}$$

where:

$$\Phi(t_k,\ t_{k-1}) = \exp(A^{*}_{k-1}\ \Delta t)$$

$$= I + A^{*}_{k-1}\ \Delta t + (A^{*}_{k-1}\ \Delta t)^{2}/2! + \ldots \tag{A.50}$$

$$\Gamma(t_k, t_{k-1}) = B^*_{k-1} \Delta t + B^*_{k-1} A^*_{k-1} \Delta t^2/2! + + B^*_{k-1} A^{*2}_{k-1} \Delta t^3/3! + \ldots \quad (A.51)$$

$$V_k = \frac{V}{\Delta t} \quad (A.52)$$

see Ref. (15). Here Δt is the discretization time interval $t_k - t_{k-1}$. Finally the covariance of the system output $\underline{z}(t_k)$ can be computed according to:

$$C_{zz}(t_k) = D^* C_{xx}(t_k) D^{*T} \quad (A.53)$$

Remark

If the atmospheric turbulence velocity components cannot be modelled as stochastic outputs of linear, low pass filters driven by gaussian, zero mean, white noise (i.e. the power spectra have a non-rational form), then an alternative method for computation of $C_{xx}(t_k)$ can be applied. Defining the variable:

$$\underline{\xi}(t) \triangleq \underline{x}(t) - D\underline{V}_g(t) \quad (A.54)$$

and rearranging eq. A.13 yields:

$$\dot{\underline{\xi}}(t) = A(t)\underline{\xi}(t) + \left[C + A(t)\, D\right] \underline{V}_g(t) \quad (A.55)$$

provided that the perturbation covariance function $C_{\underline{V}_g\underline{V}_g}(t,\tau)$ is given. The computation of $C_{\underline{\xi}\underline{\xi}}(t)$ under the latter assumption will be explained in Ref. (8).

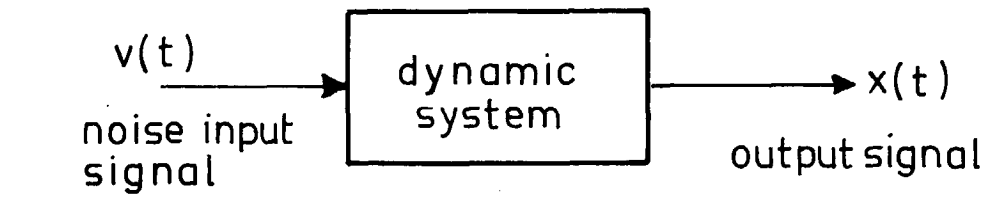

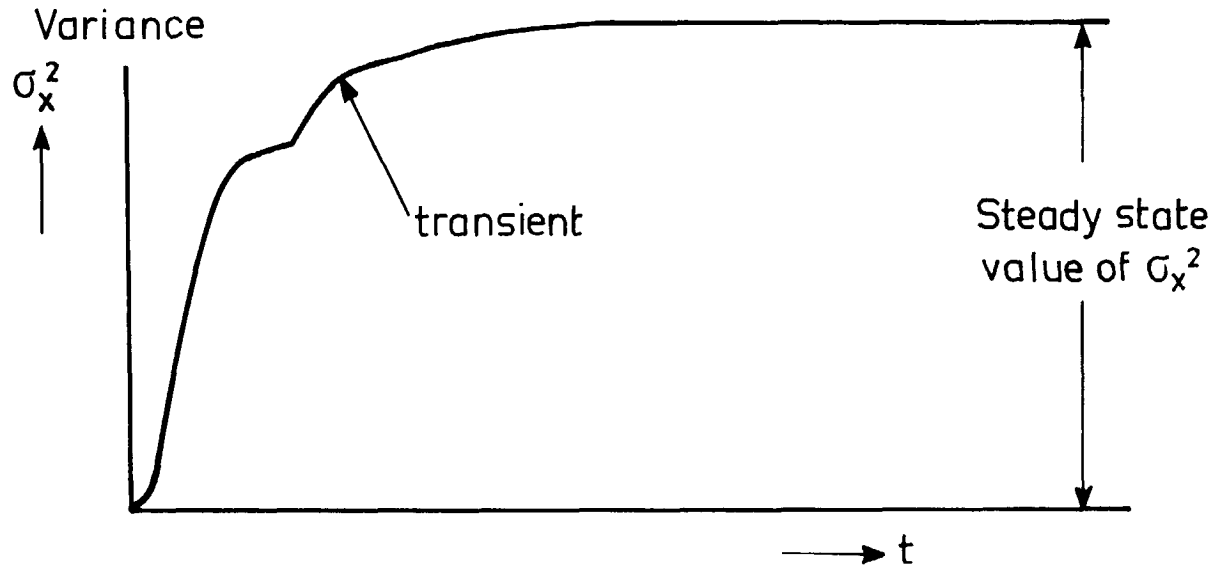

(a) Transient and steady-state response on input signal

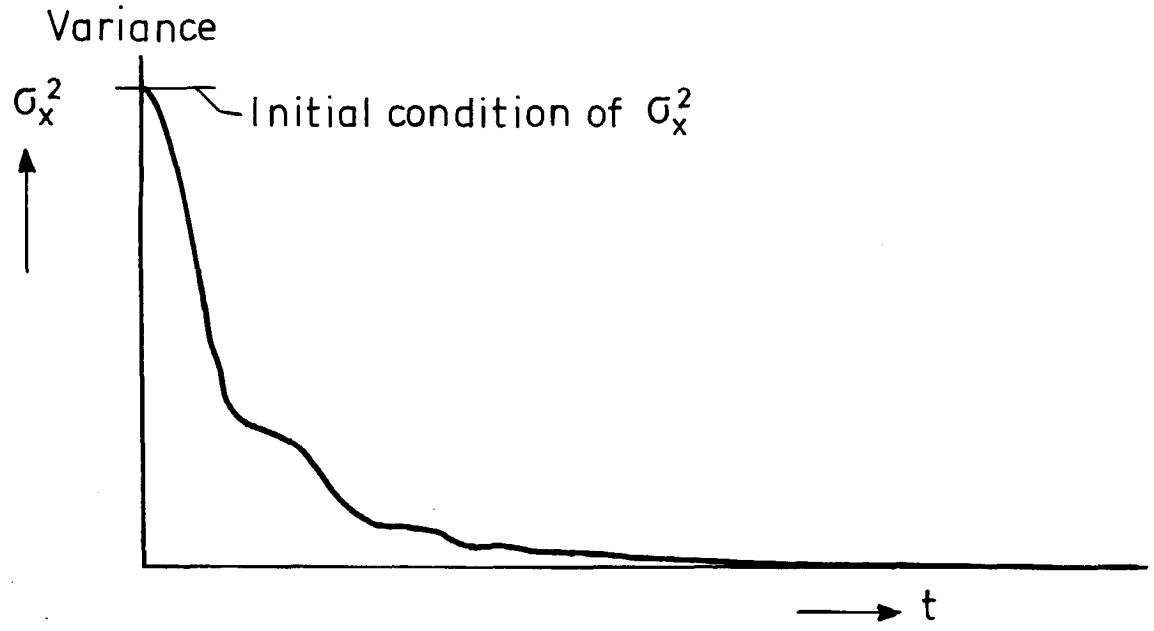

(b) Transient response on initial condition

Fig. 1. Responses of the variance on a noise input signal and on initial conditions.

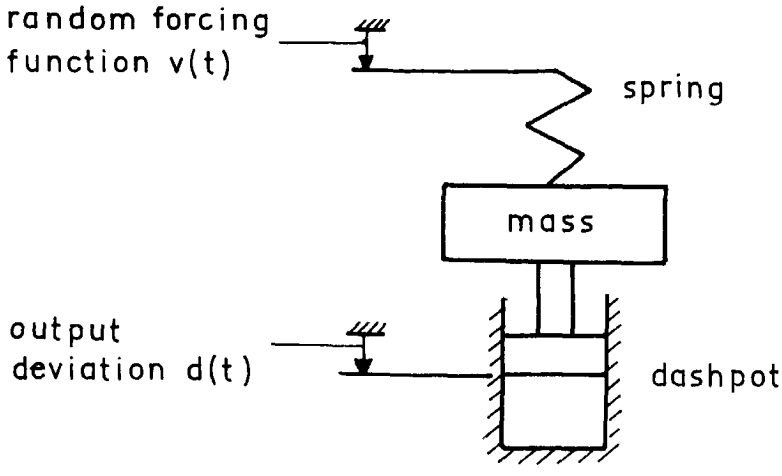

State equation : $\dot{\underline{x}}(t) = A\,\underline{x}(t) + \underline{b}\,.\,v(t)$

State vector : $\underline{x}(t) = \begin{bmatrix} x_1(t) \\ x_2(t) \end{bmatrix} = \begin{bmatrix} d(t) \\ \dot{d}(t) \end{bmatrix}$

Covariance matrix: $C_{xx}(t) = \begin{bmatrix} \sigma^2_{x_1}(t) & \sigma_{x_1x_2}(t) \\ \sigma_{x_2x_1}(t) & \sigma^2_{x_2}(t) \end{bmatrix}$

Fig. 2. Mass-spring-dashpot system of second order.

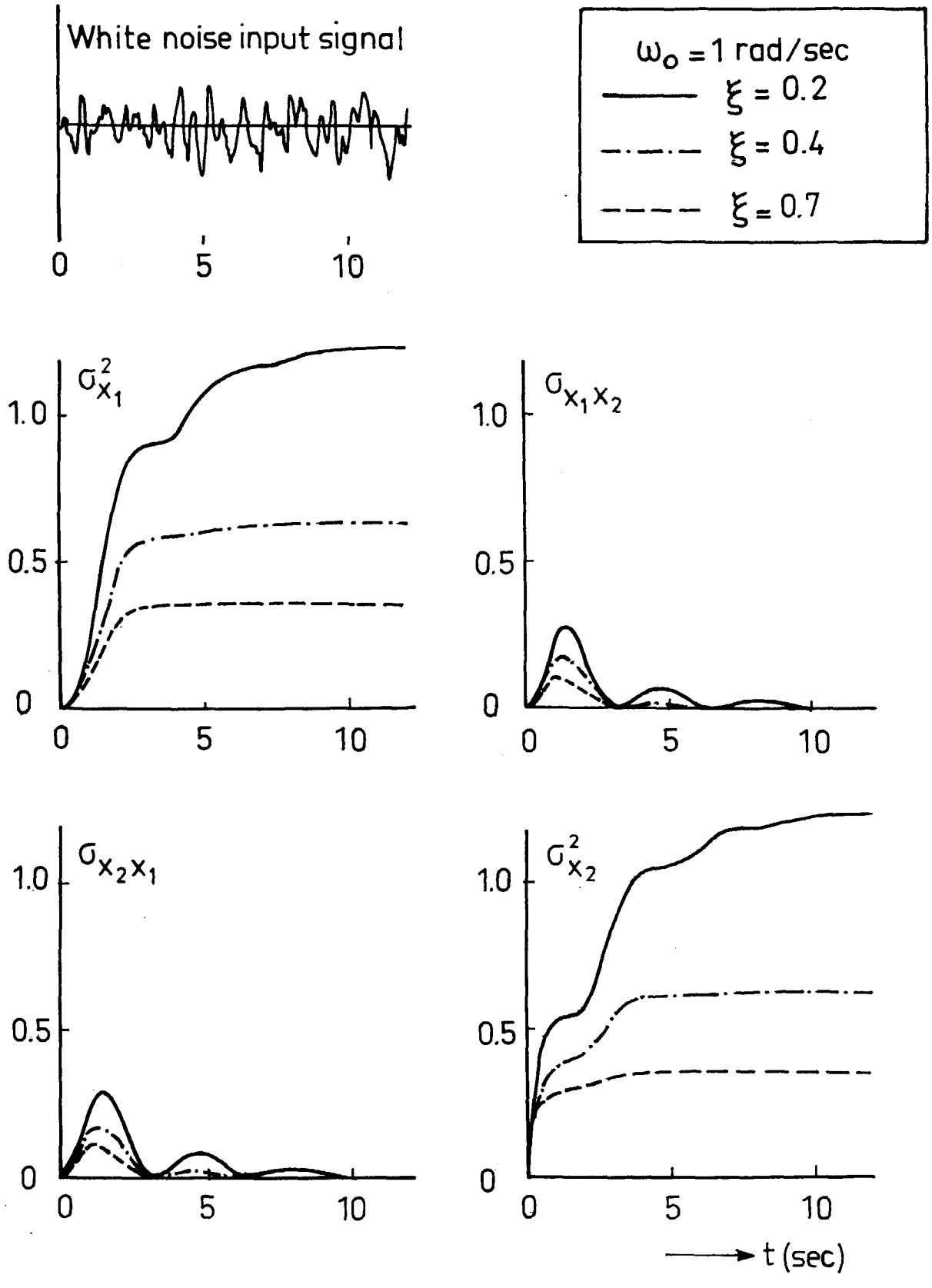

Fig. 3. Responses of the elements of the covariance matrix on a white noise input signal, initial conditions zero.

No noise input signal,
Initial conditions :

$$C_{xx}(o) = \begin{bmatrix} 1 & 0 \\ 0 & 1 \end{bmatrix}$$

$\omega_o = 1$ rad/sec
—— $\xi = 0.2$
-·-·- $\xi = 0.4$
----- $\xi = 0.7$

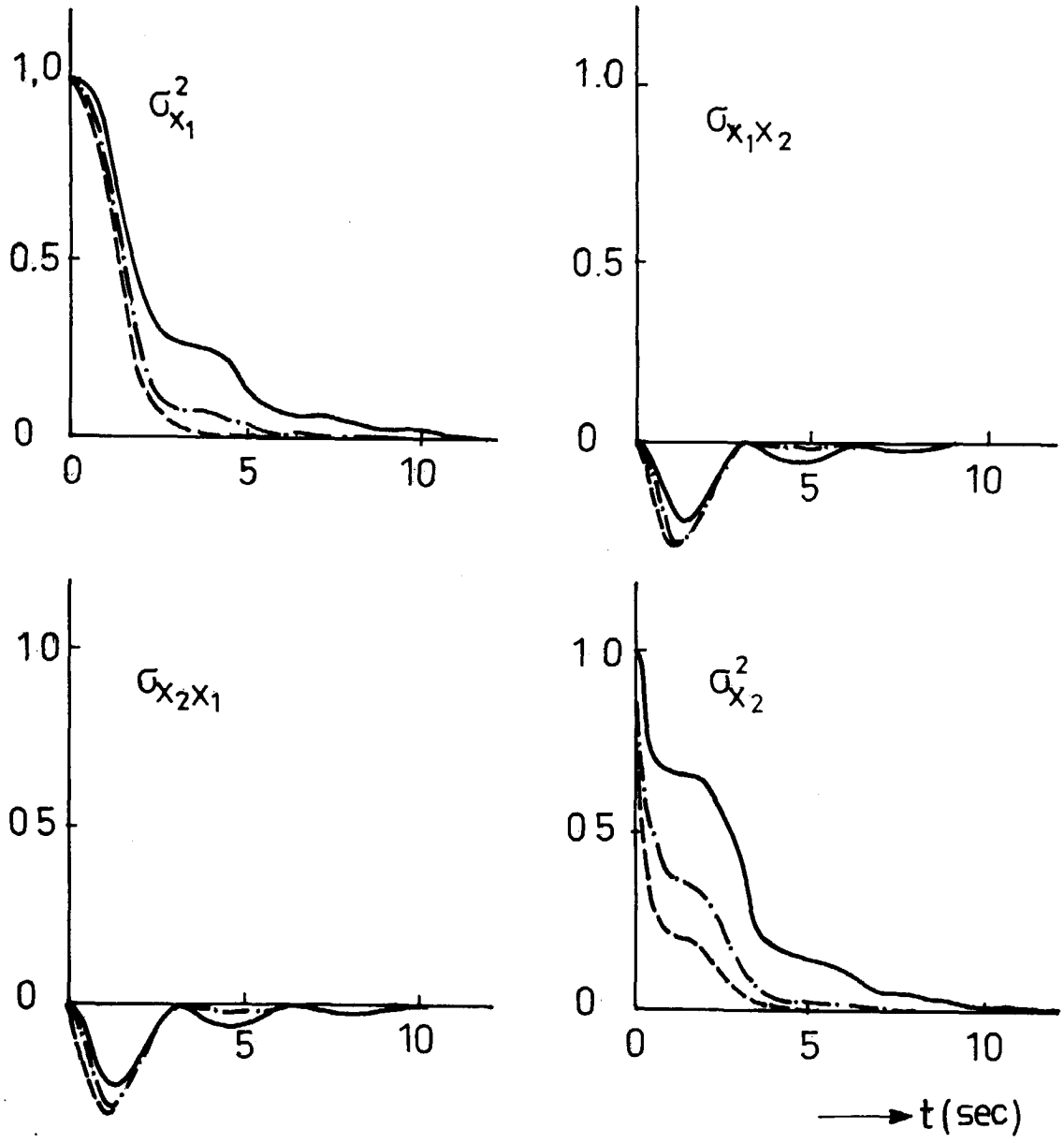

Fig. 4. Responses of the elements of the covariance matrix on initial conditions.

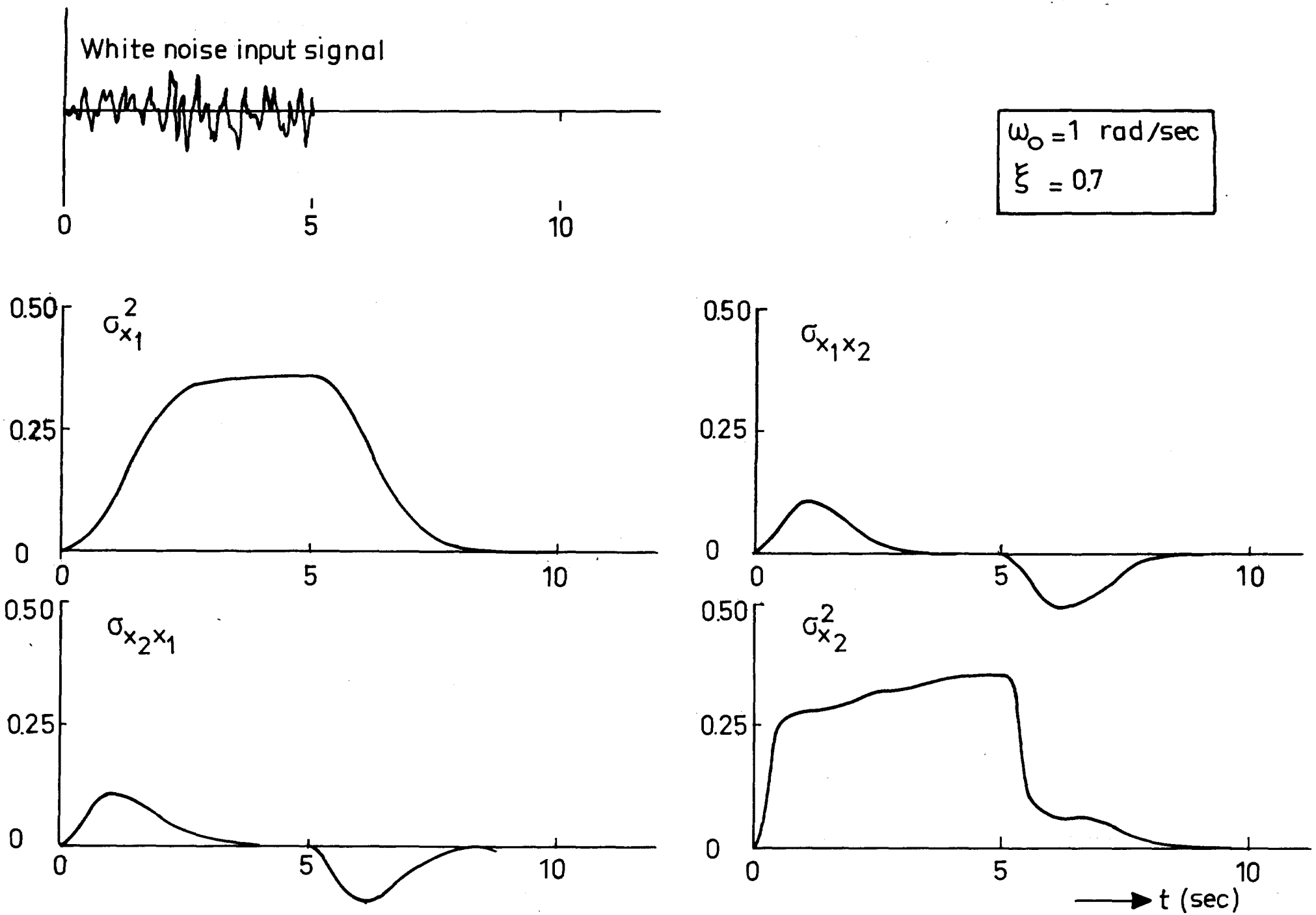

Fig. 5. Response on a white noise input signal of limited duration.

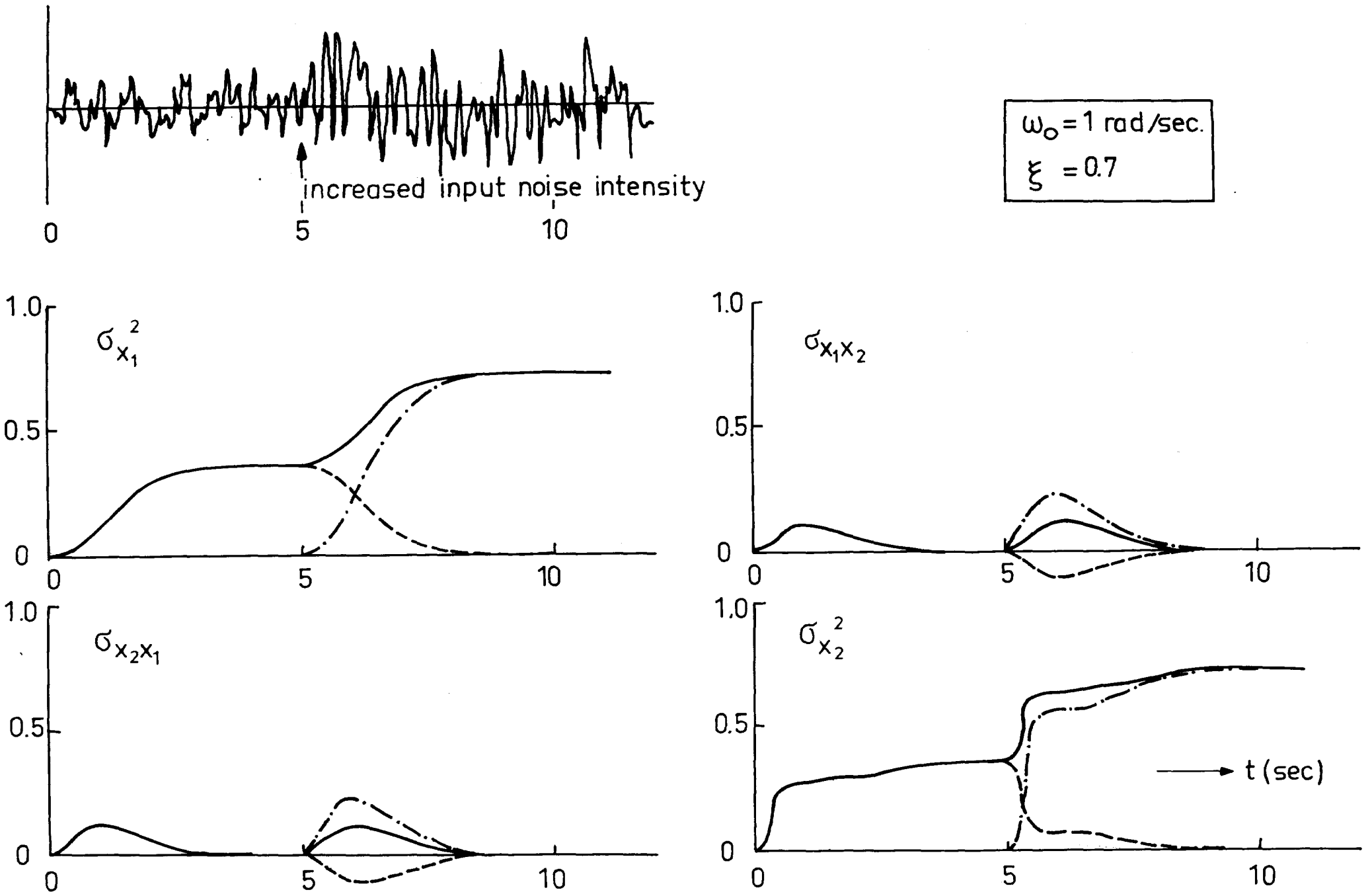

Fig. 6. The effect of a stepwise increase in white noise input intensity.

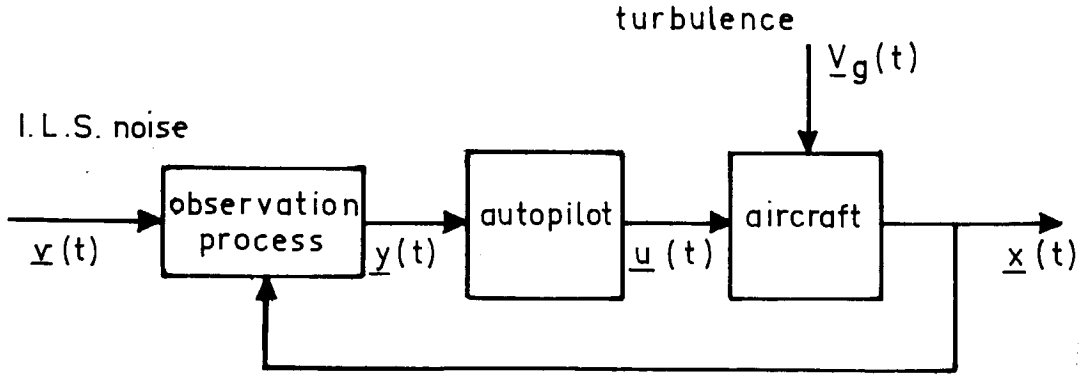

(a) Controlled aircraft perturbed by coloured noise processes

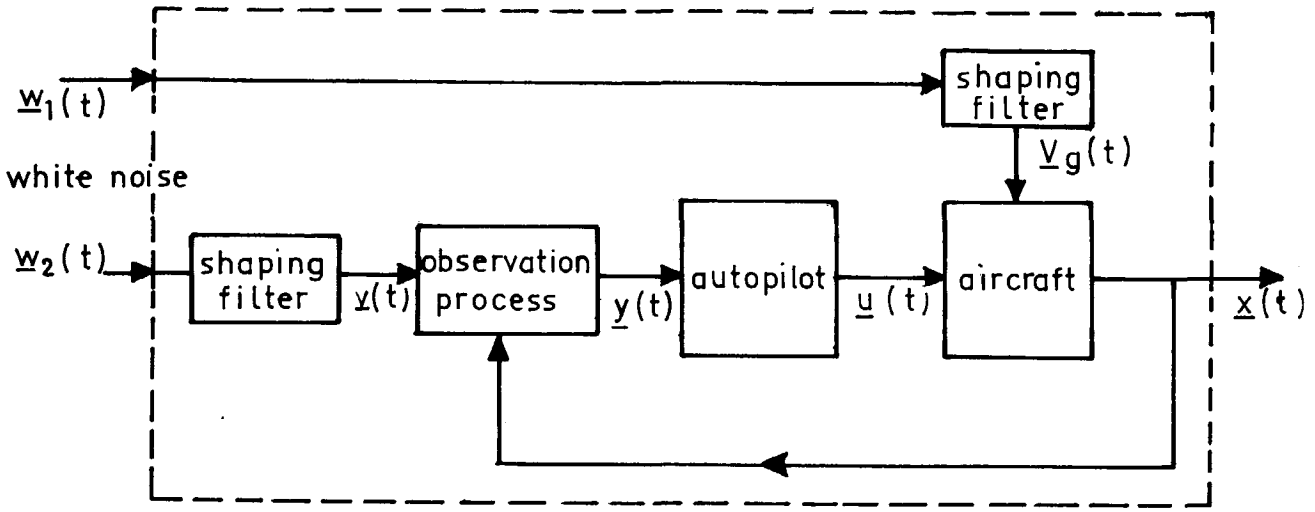

(b) Addition of shaping filters

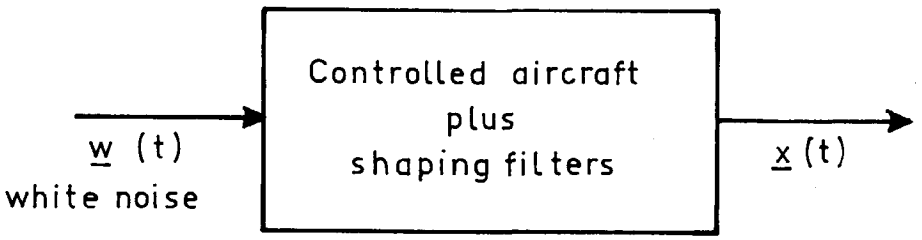

(c) Controlled aircraft and shapingfilters as one system perturbed by white noise
State equation :

$$\dot{\underline{x}}(t) = A\underline{x}(t) + B\underline{w}(t)$$

Fig. 8. Block diagrams of shaping filters and controlled aircraft.

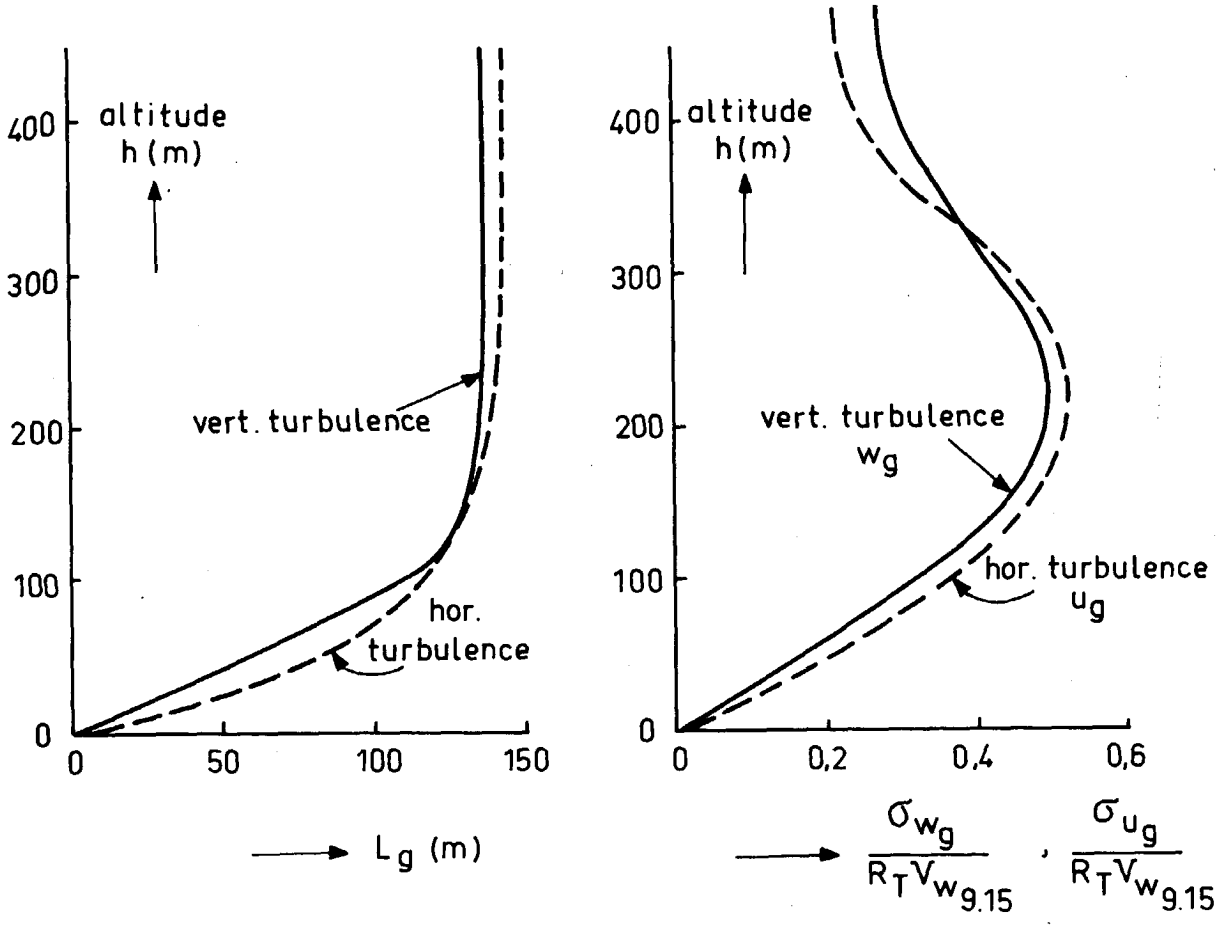

Fig. 9. Integral scale lengths and intensities of low altitude atmospheric turbulence according to Pritchard (see Ref. 10). Neutral atmosphere.

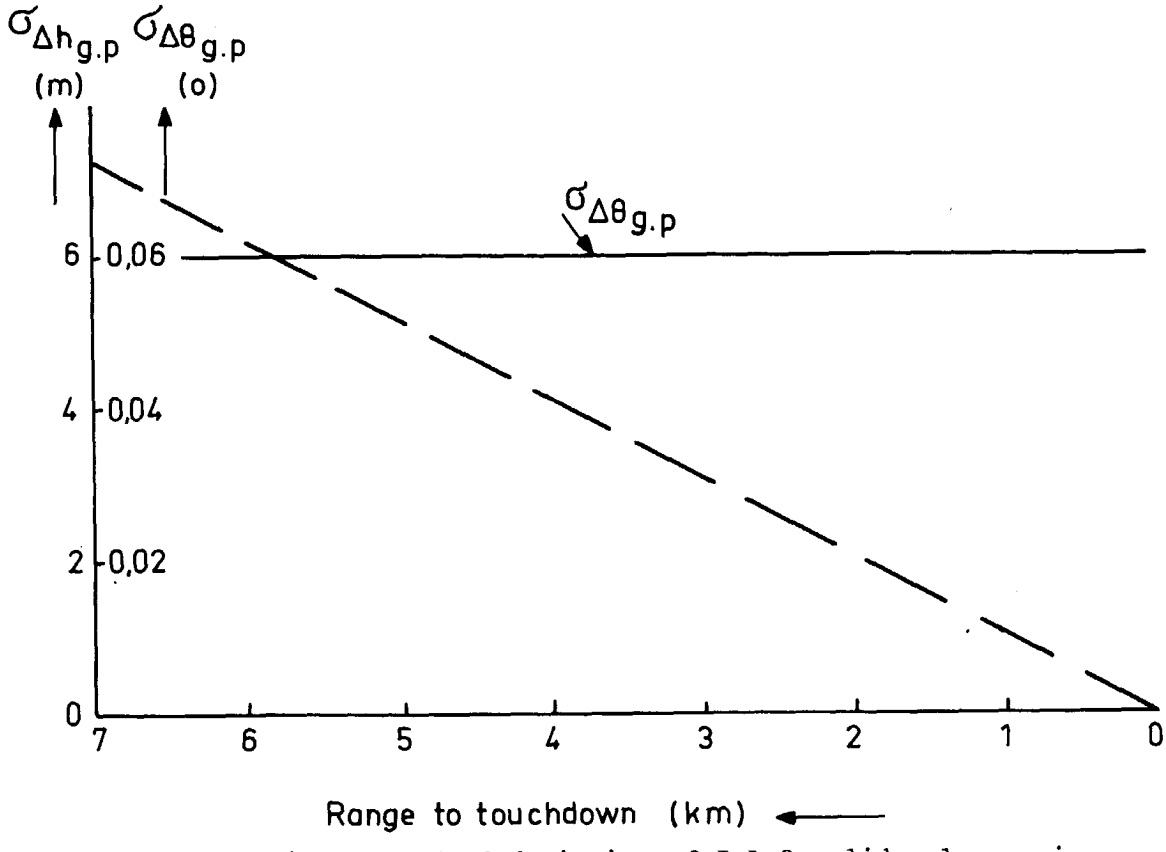

Fig. 10. Maximum standard deviation of I.L.S. glide slope noise expressed in angular deviation ($\Delta\theta_{g.p}$) and altitude deviation (Δhg.p) (Ref. 10).

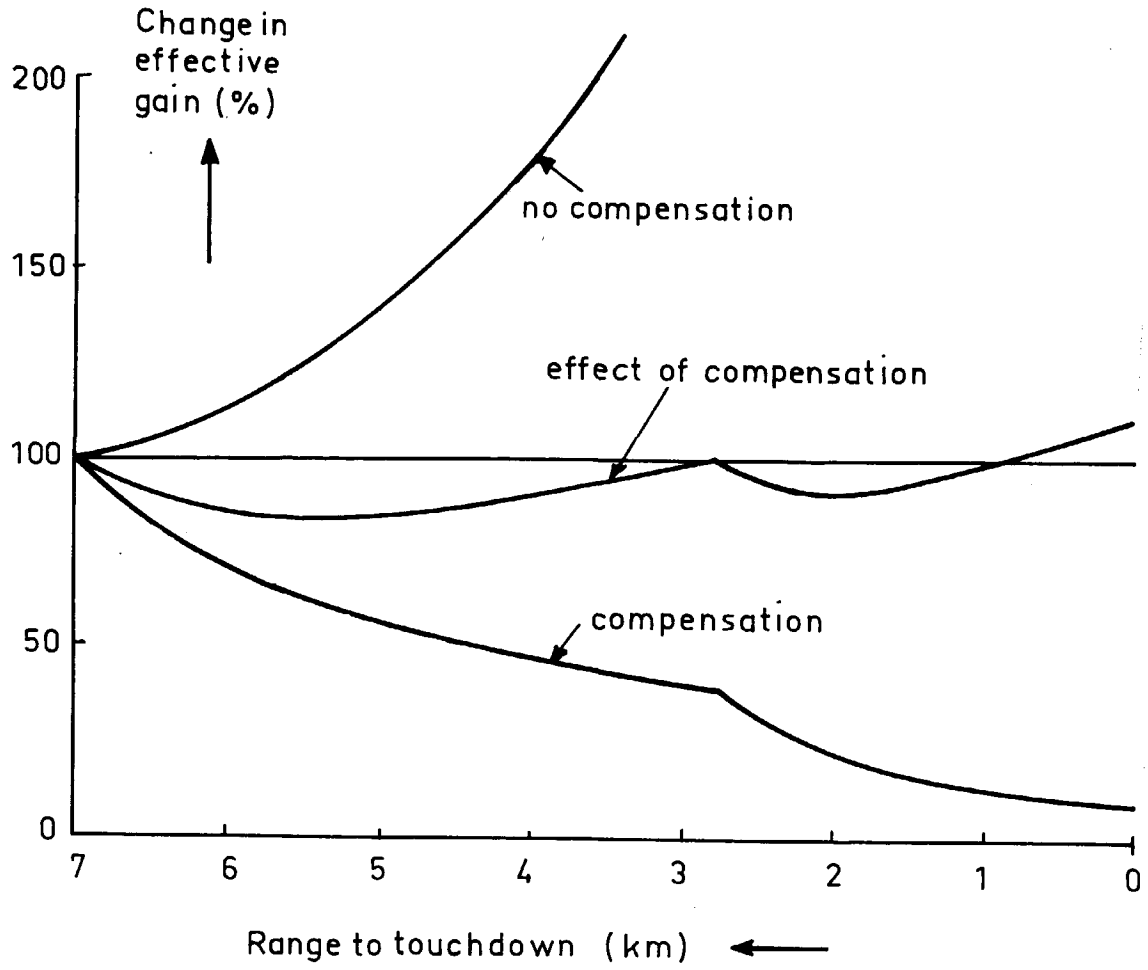

Fig. 11. Change in effective gain (elevator angle per unit altitude deviation) due to glide path geometry. Effect of compensation.

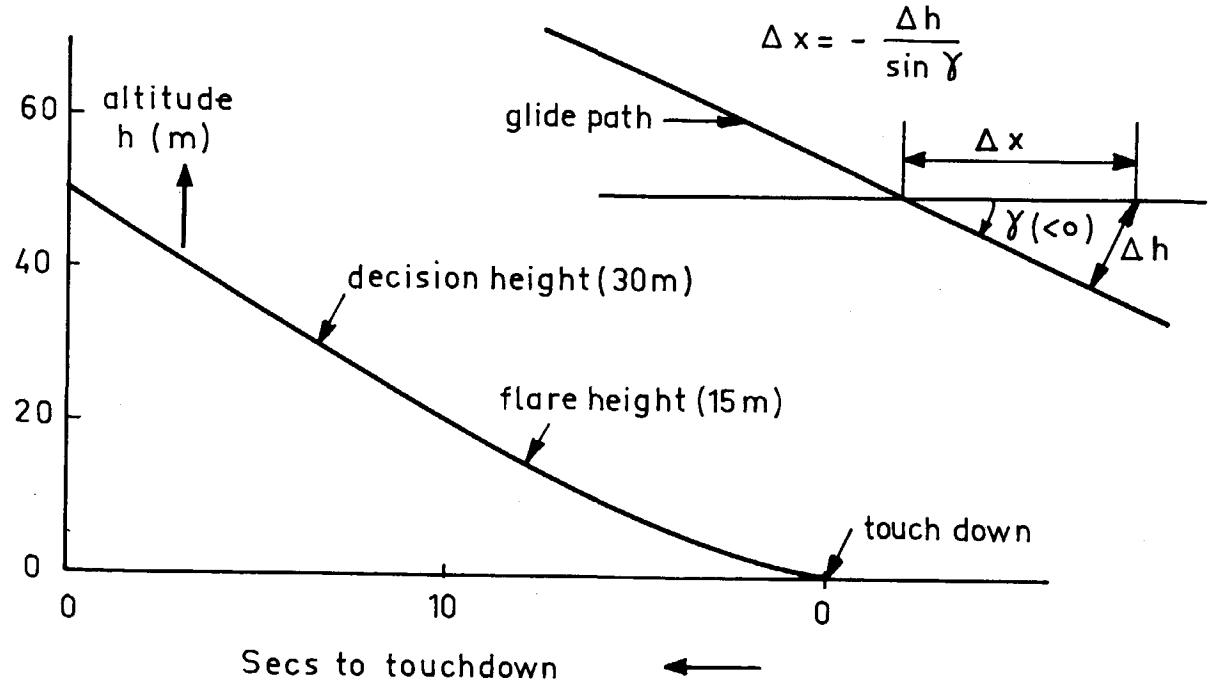

Fig. 12. Effect of deviations Δh relative to the glide path on deviations Δx in distance along the runway.

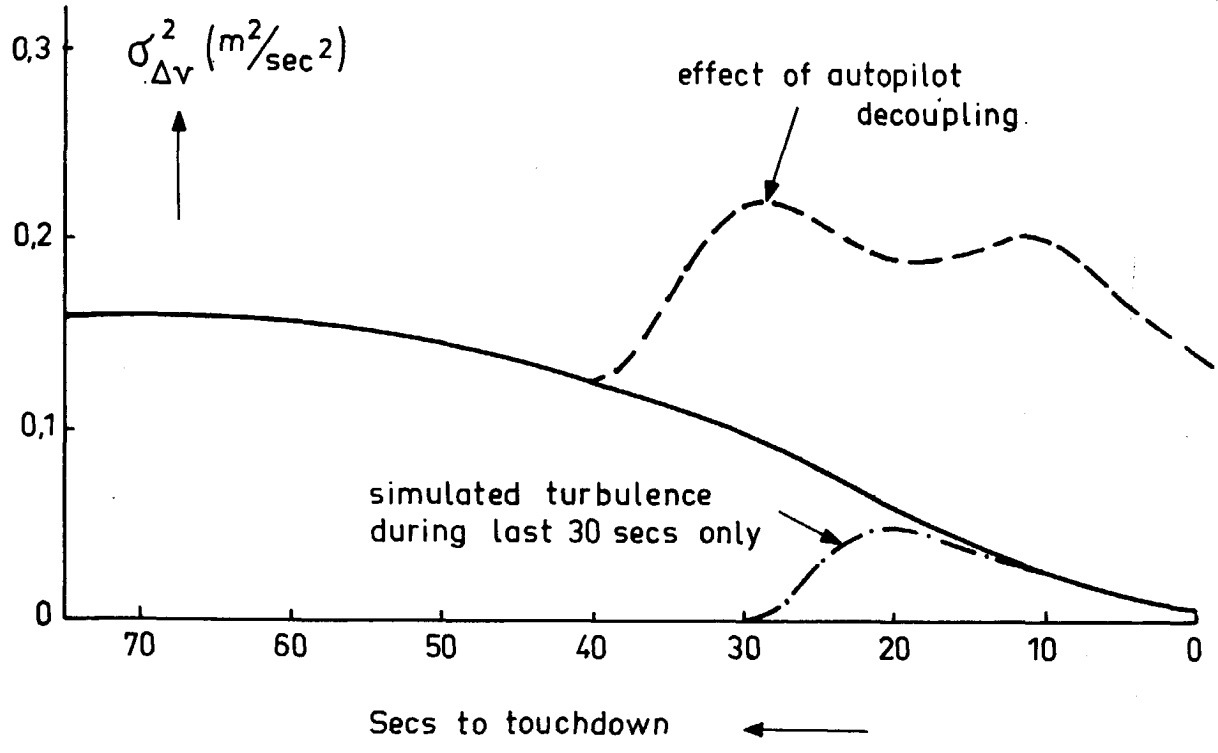

Fig. 13. Variance of deviations in flight speed due to turbulence during an approach. Neutral atmosphere, $V_{w_{9.15}}$ = 1 m/sec.

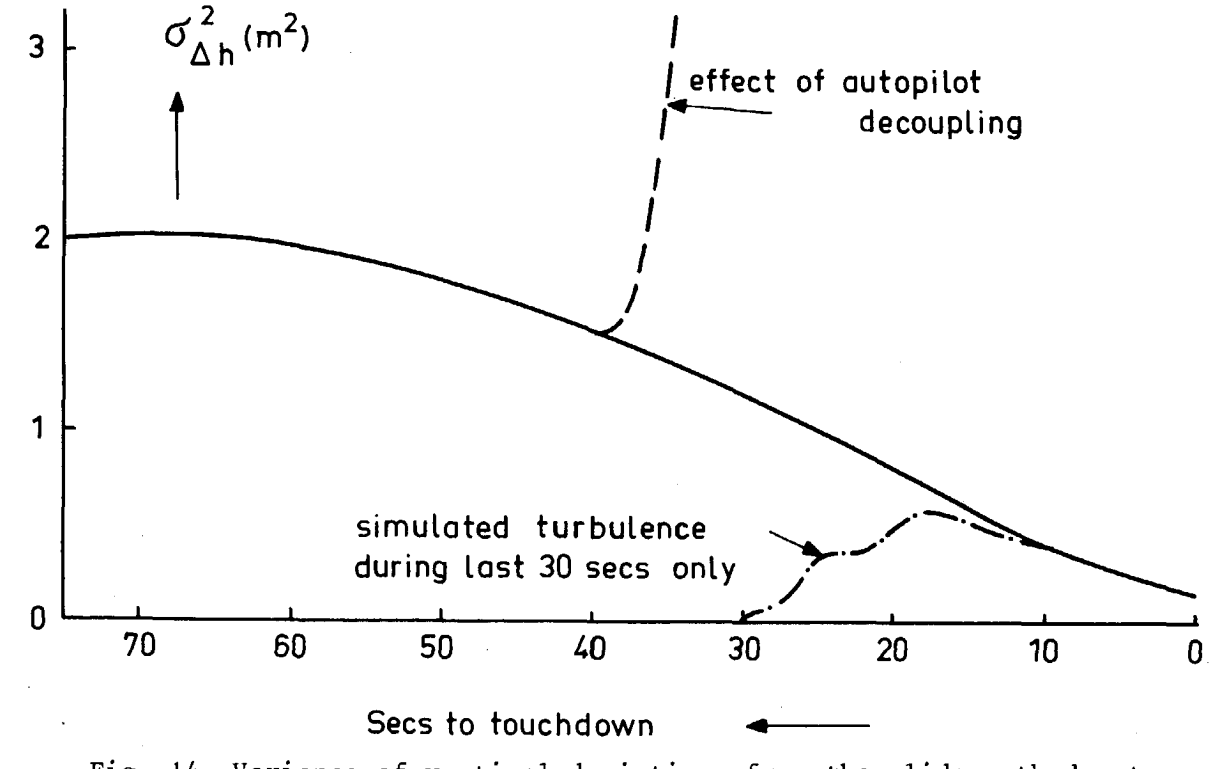

Fig. 14. Variance of vertical deviations from the glide path due to turbulence. Neutral atmosphere, $V_{w_{9.15}}$ = 1 m/sec.

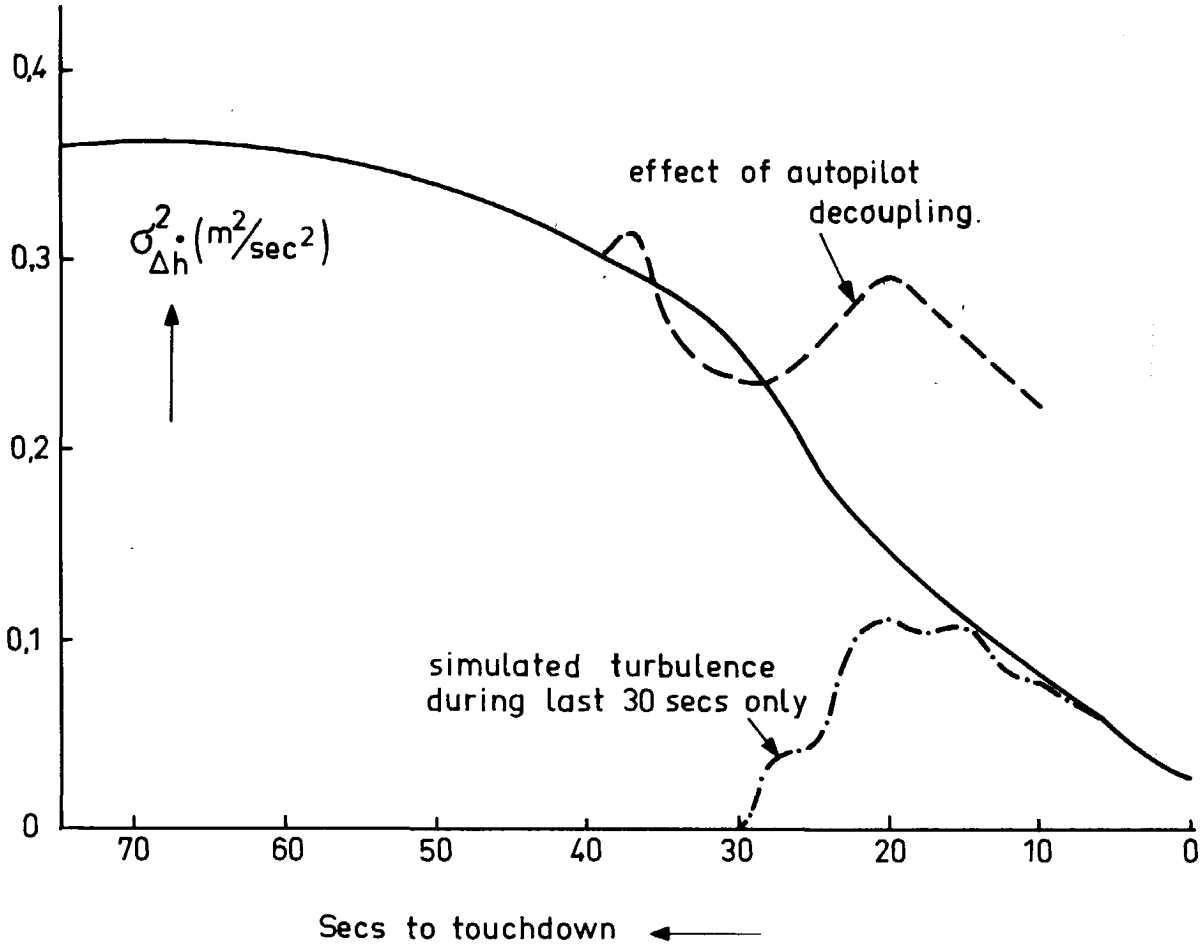

Fig. 15. Variance of sink rate due to turbulence. Neutral atmosphere, $V_{w_{9.15}}$ = 1 m/sec.

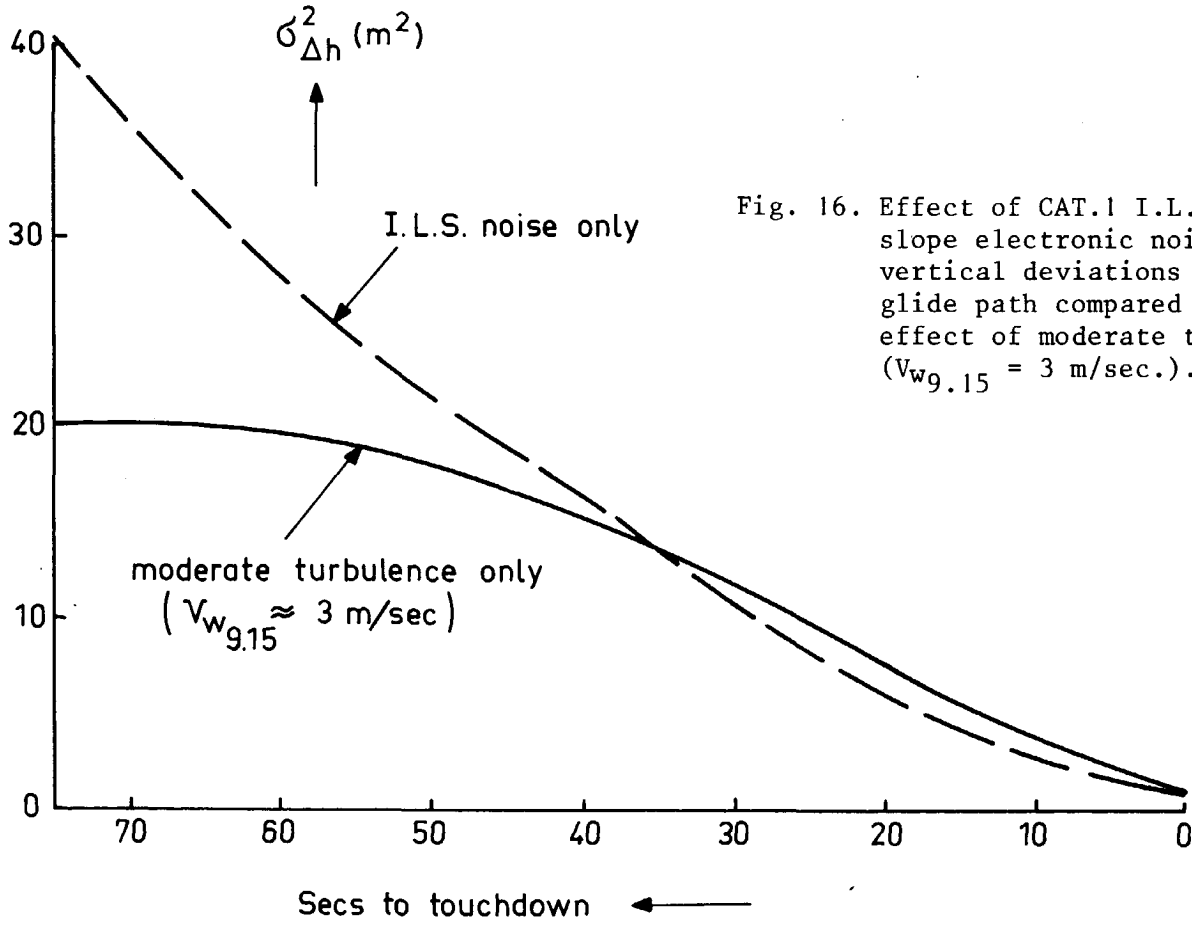

Fig. 16. Effect of CAT.1 I.L.S. glide slope electronic noise on vertical deviations from the glide path compared with the effect of moderate turbulence ($V_{w_{9.15}}$ = 3 m/sec.).

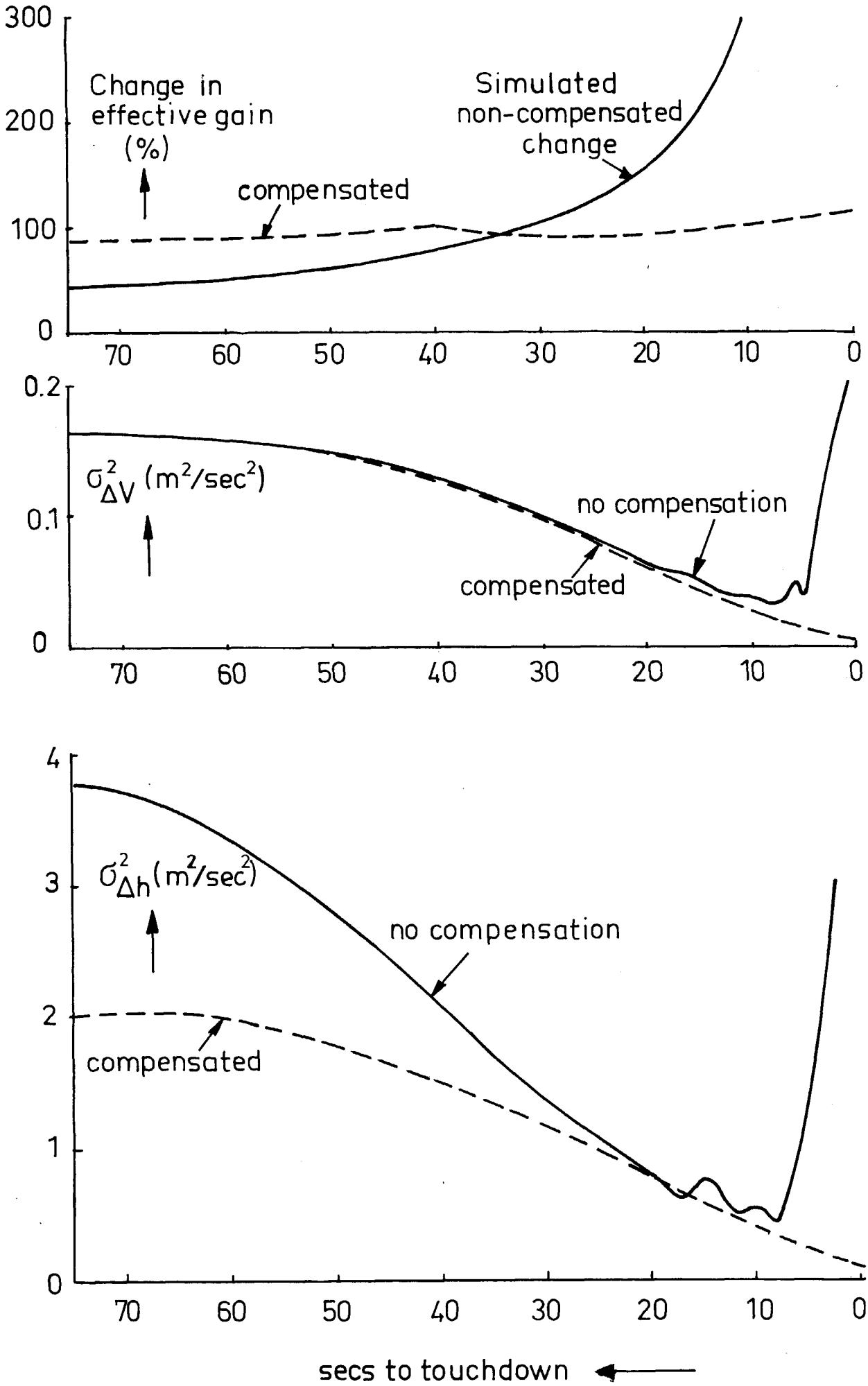

Fig. 17. Variance of deviations in flight speed and deviations from the glide path for non-compensated changes in effective gain due to I.L.S. beam geometry.

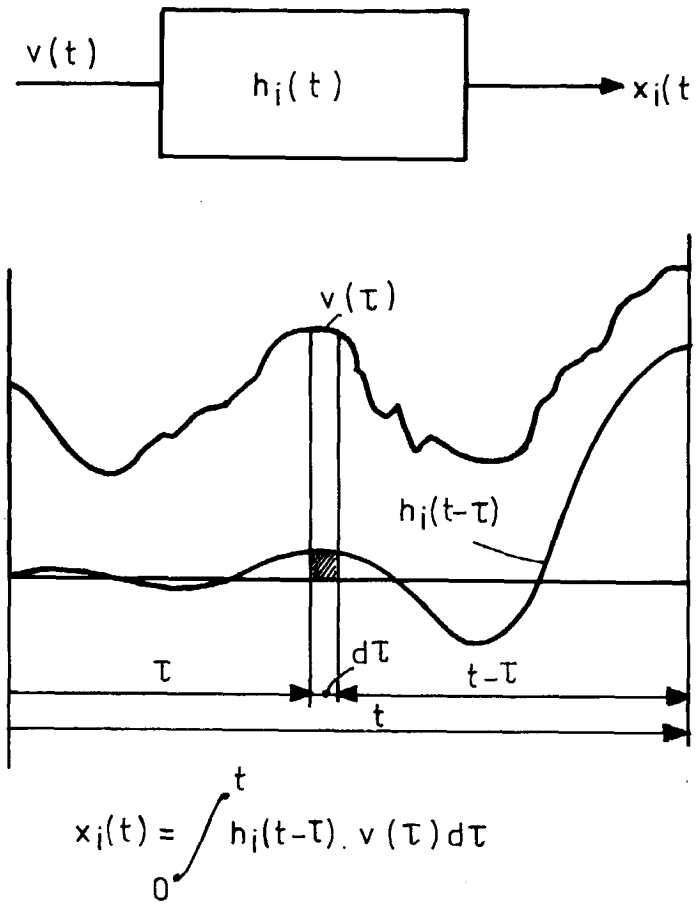

Fig. 18. Convolution integral of $h(t - \tau)$ and $v(\tau)$ representing the contribution of $v(\tau)$ for $0 \leq \tau \leq t$ to $x(t)$.

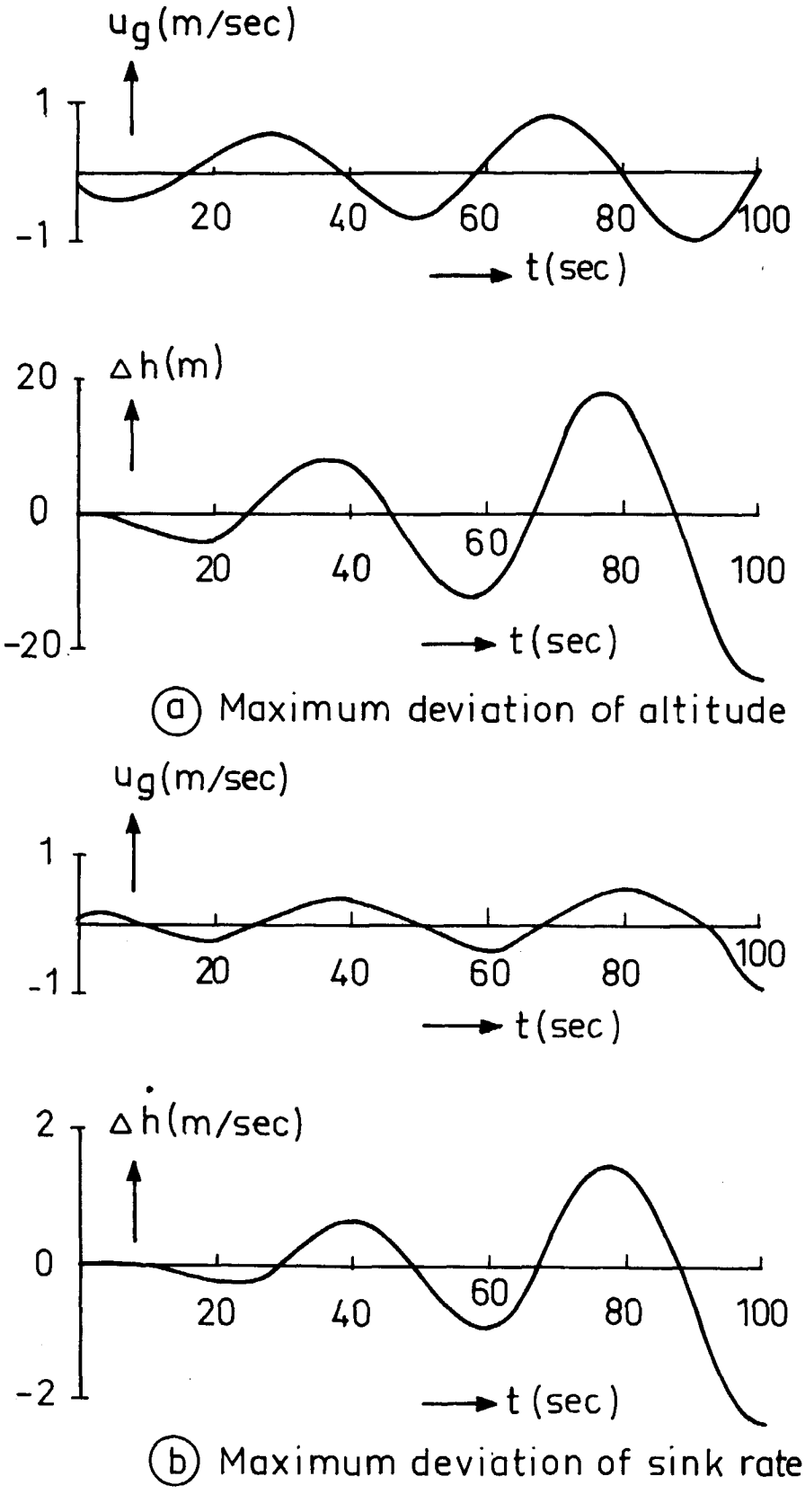

ⓐ Maximum deviation of altitude

ⓑ Maximum deviation of sink rate

Fig. 19. Worst case time-histories of horizontal wind speed and resulting maximum deviations of altitude and sink rate at t = 100 sec. Unstabilized aircraft, approach configuration.

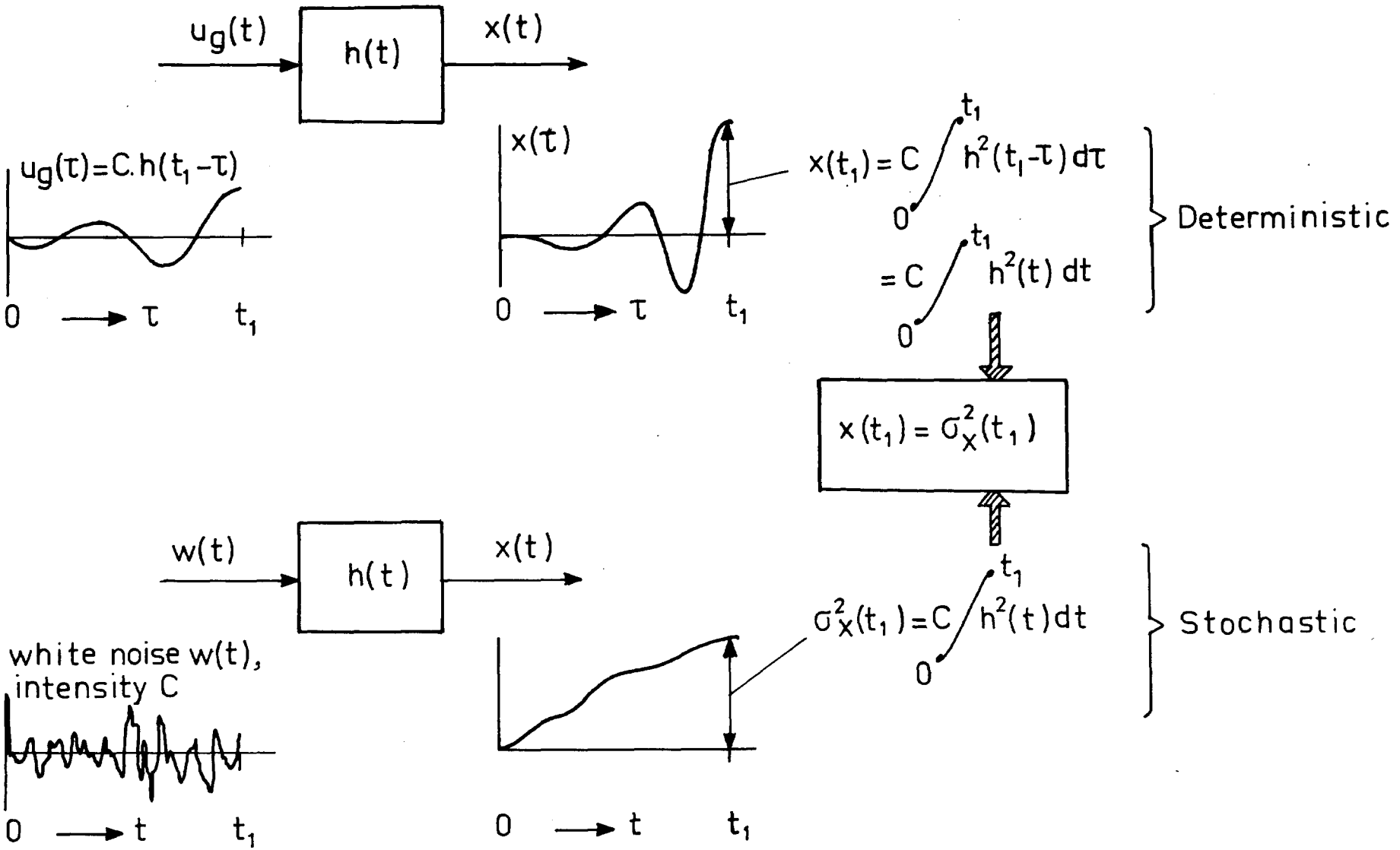

Fig. 20. Relation between maximum deviation x at t_1 (worst case, deterministic) and the variance $\sigma_x^2(t_1)$ of x(t) in the white noise driven stochastic case.